

# Hamburger Geophysikalische Einzelschriften

Herausgegeben von den Geophysikalischen Instituten der Universität Hamburg  
und dem Max-Planck-Institut für Meteorologie  
(Fachgebiete: Meteorologie, Ozeanographie, Physik des Erdkörpers)

---

Reihe A: Wissenschaftliche Abhandlungen

Heft 74

## Calculation of the Nonlinear Wave-Wave Interactions in Cross Seas

von

I.R. Young

S. Hasselmann

K. Hasselmann

Hamburg 1985

G. M. L. WITTENBORN SÖHNE  
2000 HAMBURG 13

Preis 18,— DM

2  
Hann M

AUS DEM MAX-PLANCK INSTITUT FÜR METEOROLOGIE

H A M B U R G

Max-Planck-Institut für Meteorologie  
Hamburger Geophysikalische Einzelschriften

# Hamburger Geophysikalische Einzelschriften

Herausgegeben von den Geophysikalischen Instituten der Universität Hamburg  
und dem Max-Planck-Institut für Meteorologie  
(Fachgebiete: Meteorologie, Ozeanographie, Physik des Erdkörpers)

Reihe A: Wissenschaftliche Abhandlungen

Heft 74

## Calculation of the Nonlinear Wave-Wave Interactions in Cross Seas

von

I.R. Young

S. Hasselmann

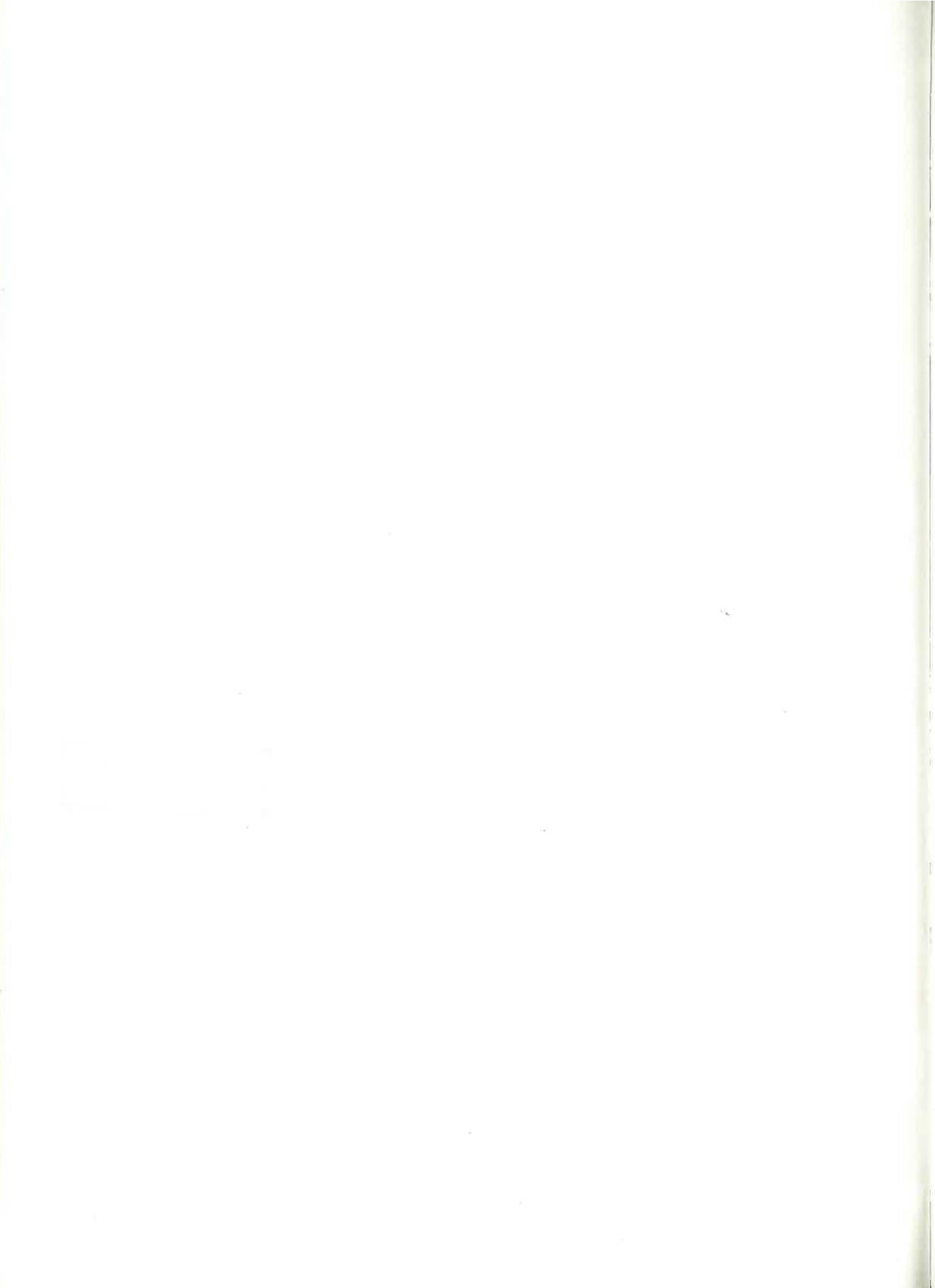
K. Hasselmann



Hamburg 1985

G. M. L. WITTENBORN SOHNE  
2000 HAMBURG 13

Preis 18,— DM



# Calculations of the Nonlinear Wave-Wave Interactions in Cross Seas

I.R. Young (1)

S. Hasselmann (2)

K. Hasselmann (2)

## 1. Introduction

It has long been realized that one of the most significant processes in determining the rate of growth of ocean waves and particularly the shape of the spectrum is nonlinear wave-wave interactions. The complexity of the Boltzmann integral expression (K. Hasselmann, 1961), however, has meant that solutions by traditional integration techniques have been computationally very expensive. Hasselmann and Hasselmann (1981, 1985) have developed a much more efficient solution technique which takes advantage of the symmetric properties of the integrand by introducing symmetric variables. Additional savings are made by precomputing the integral grid and the interaction coefficients and filtering out unimportant regions of the phase space.

The added efficiency of this computation technique has made possible the compilation of data sets of nonlinear transfers for various spectral shapes. Hasselmann and Hasselmann (1981) investigated the nonlinear transfer for spectra conforming to the general JONSWAP form but with

---

(1) James Cook University of North Queensland, Townsville, Australia

(2) Max-Planck-Institut für Meteorologie, Hamburg, FRG

varying spectral parameters. Such data sets prove invaluable, not only in providing input to subsequent parameterizations, but also in increasing physical understanding of the interaction process.

In the present work these calculations are extended to investigate the interactions for seas with two spectral peaks. These peaks can be separated in both frequency and direction. Thus it is possible to investigate the nonlinear coupling in cross sea conditions which may occur, for example, as the result of the passage of a frontal system. The correct simulation of such complex seas is one of the most critical tests of a wave model (cf. SWAMP Group, 1985).

## 2. Cases computed

All spectra considered consisted of the superposition of two directional spectra  $E(f, \sigma)$ , each of which was represented by a JONSWAP frequency spectrum

$$E(f) = \alpha g^2 (2\pi)^{-4} f^{-5} \exp\left\{-\frac{5}{4}[f/f_m]^4\right\} \exp\{\ln\gamma \exp[-\frac{(f-f_m)^2}{2\sigma^2 f_m^2}]\}$$

with  $\sigma = \begin{cases} \sigma_a \\ \sigma_b \end{cases}$  for  $f \begin{cases} < f_m \\ > f_m \end{cases}$

multiplied by a spreading function of the form (D. Hasselmann, 1980)

$$S(f, \theta) = I(p)^{-1} \cos^{2p} (\theta - \theta_m)/2 \quad (1)$$

where  $\theta_m$  is the mean propagation direction,

$$p = 9.77(f/f_m)^\beta$$

$$\beta = \begin{cases} 4.06 & \text{for } f < f_m \\ -2.34 & \text{for } f \geq f_m \end{cases}$$

and the normalization factor is given by

$$I(p) = \frac{2^{(1-2p)} \cdot \pi \cdot \Gamma(2p+1)}{\Gamma^2(p+1)}$$

A total of 21 cases were considered. The mean angle of the first spectrum was set at  $0^\circ$ , while for the second spectrum  $\theta_m$  varied between  $0^\circ$  and  $180^\circ$ . The first spectrum always had the standard JONSWAP parameters  $\alpha = 0.01$ ,  $\gamma = 3.3$ ,  $\sigma_a = 0.07$ ,  $\sigma_b = 0.09$  with  $f_m = 0.3$  Hz. The parameters for the second spectrum are shown in Table 1.

The values of  $\alpha$  were selected such that if the sub-spectra acted independently of each other, they would have nonlinear transfers of similar magnitude, irrespective of their  $f_m$  values. The  $\alpha$ -values were calculated from the general scaling relationship for  $S_{nl}$ , which states that for a spectrum of the form

Run. No.	$\theta_m$	$f_m$ (Hz)	$\alpha$
1	0°	0.3	0.010
2	30°	0.3	0.010
3	60°	0.3	0.010
4	90°	0.3	0.010
5	120°	0.3	0.010
6	150°	0.3	0.010
7	180°	0.3	0.010
8	0°	0.4	0.0147
9	30°	0.4	0.0147
10	60°	0.4	0.0147
11	90°	0.4	0.0147
12	120°	0.4	0.0147
13	150°	0.4	0.0147
14	180°	0.4	0.0147
15	0°	0.5	0.0198
16	30°	0.5	0.0198
17	60°	0.5	0.0198
18	90°	0.5	0.0198
19	120°	0.5	0.0198
20	150°	0.5	0.0198
21	180°	0.5	0.0198

Table 1: Parameters of second sub-spectra in full spectrum for each test case. In each case  $\gamma = 3.3$  and  $\sigma_a = 0.07$ ,  $\sigma_b = 0.09$ .

$$E(f, \theta) = \alpha g^2 f_m^{-5} \Phi(f/f_m, \theta)$$

the nonlinear transfer is given by

$$S_{nl}(f, \theta) = \alpha^3 g^{-2} f_m^{-4} \psi(f/f_m, \theta) \quad (2)$$

### 3. Results

Figures 1 - 21 show the spectra and resulting nonlinear transfers for each of the cases of Table 1. The computations were carried out with a logarithmic frequency resolution  $\Delta f/f = 0.1$  and  $30^\circ$  angular resolution. Part (a) of each figure represents the spectrum and part (b) its nonlinear transfer. Values are shown as a function of frequency at  $30^\circ$  intervals from  $0^\circ$  to  $330^\circ$ .  $0^\circ$  appears in the top left corner with  $30^\circ$  below it and  $60^\circ$  below that. The second column begins with  $90^\circ$ ; other angles follow in similar fashion. The plots of the nonlinear transfer,  $S_{nl}$ , show both the full transfer (solid line) and the summed transfer which would result if the two seas acted completely independently (dashed line). Hence, a comparison between the dashed and solid lines gives a clear indication of the coupling between the two seas.

Cases 1 - 7 represent the superposition of spectra with the same peak frequencies but different mean directions. When both spectra

are at  $0^\circ$ , the effect is identical to doubling the value of  $\alpha$  (cf. Fig. 1). This yields an eightfold increase of the nonlinear transfer (cf. eq. (2)), or a fourfold increase over the result obtained by simply summing the transfers. However, as the directional separation between the two spectra increases, the nonlinear coupling gradually decreases, and for angles of  $90^\circ$  and greater the coupling is virtually negligible.

The remaining cases represent spectra separated in both frequency and direction. Our choice of scaling implies that the magnitude of the high frequency sub-spectrum is significantly less than that of the low frequency sub-spectrum. Thus the high frequency peak appears as a relatively small anomaly on the otherwise standard spectral shape. The nonlinear transfer has a twofold response to this bi-model spectral distribution. Firstly, the coupling between the two spectra causes an amplification of the transfer. This amplification decreases as the spectral peaks become more separated in both frequency and direction. The actual shape of the transfer is, however, also considerably modified in comparison with the summation of the individual transfers. The negative lobe of the high frequency transfer is significantly enhanced. Such a nonlinear transfer would result in a rapid decay of the high frequency sea. The nonlinear transfers appear to favour a uni-model JONSWAP type spectral distribution and act to force the spectrum back to this preferred shape.

References

Hasselmann, K. (1961), On the nonlinear energy transfer in a gravity wave spectrum. 1: General theory. J.Fluid Mech. 12, 481-500.

Hasselmann, K., T.P. Barnett, E. Bouws, H. Carlson, D.E. Cartwright, K. Enke, J.A. Ewing, H. Gienapp, D.E. Hasselmann, P. Kruseman, A. Meerburg, P. Müller, D.J. Olbers, K. Richter, W. Sell, and H. Walden (1973), Measurements of wind-wave growth and swell decay during the Joint North Sea Wave Project (JONSWAP). Deutsche Hydrogr. Z. A(8<sup>0</sup>), No. 12.

Hasselmann, S., and K. Hasselmann (1981), A symmetrical method of computing the nonlinear transfer in a gravity wave spectrum. Hamburger Geophysikalische Einzelschriften, Reihe A: Wissenschaftliche Abhandlungen, Heft 52.

Hasselmann, S., and K. Hasselmann (1985), Computations and parameterizations of the nonlinear energy transfer in a gravity wave spectrum. Part 1: A new method for efficient computations of the exact nonlinear transfer integral (submitted to J.Phys.Oceanogr.)

SWAMP Group (1985), Ocean Wave Modeling. Plenum Press, New York, 256 pp.

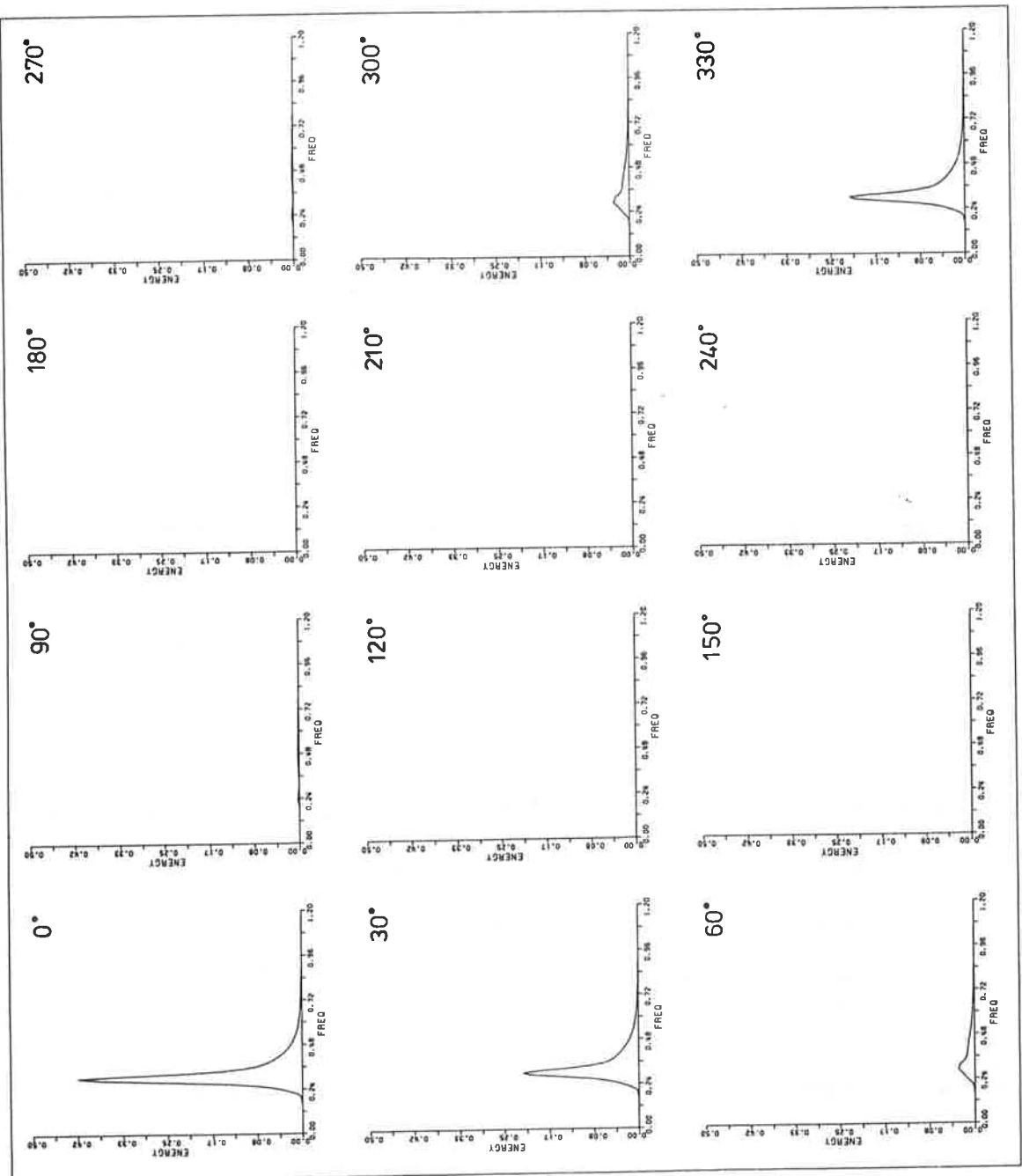


Fig. 1a  $E(f, \theta)$ :  $f_{1m} = 0.3\text{Hz}$ ,  $\theta_{1m} = 0^\circ$ ,  $f_{2m} = 0.3\text{Hz}$ ,  $\theta_{2m} = 0^\circ$

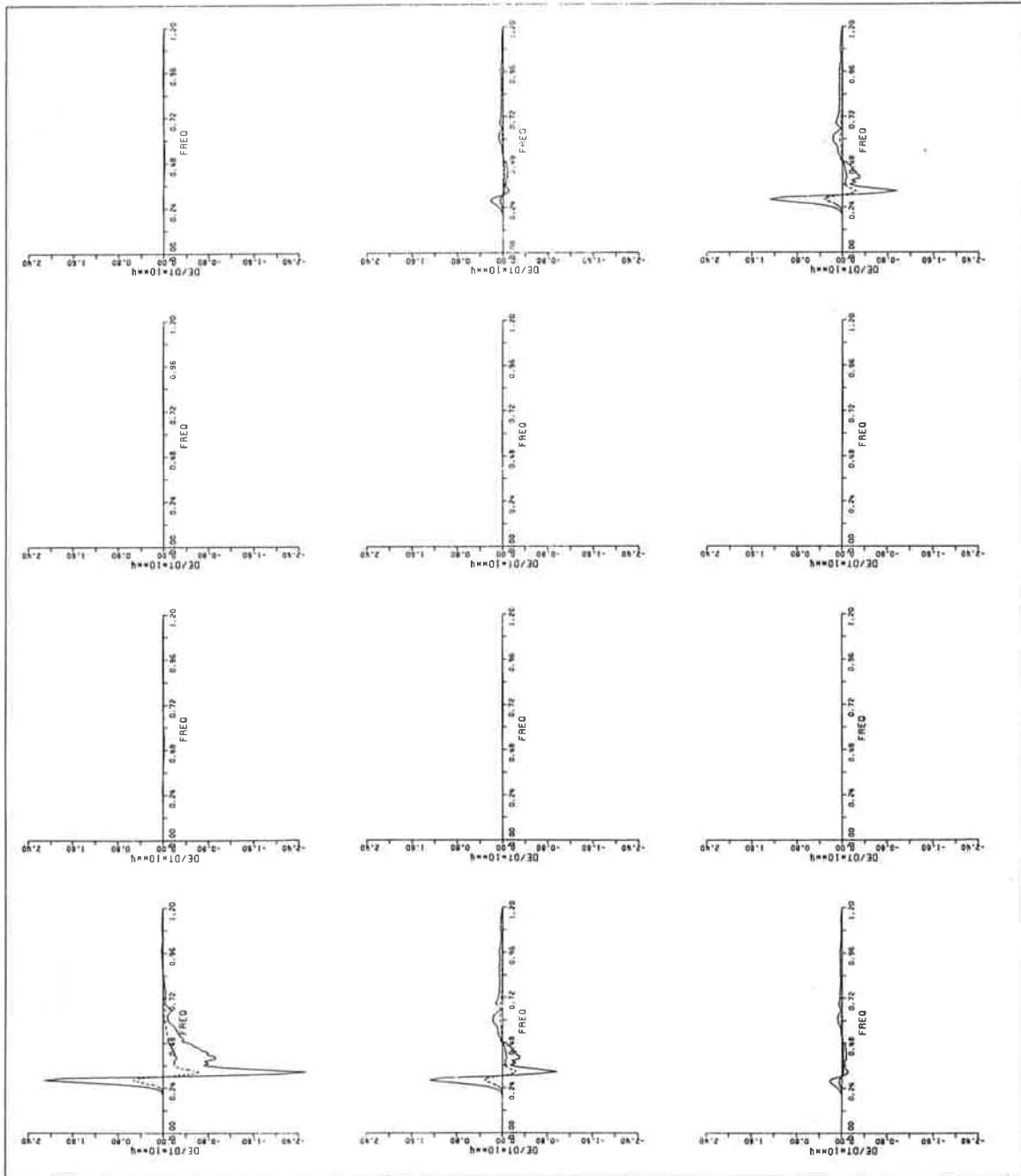


Fig. 1b  $S_{n1}(f, \theta)$

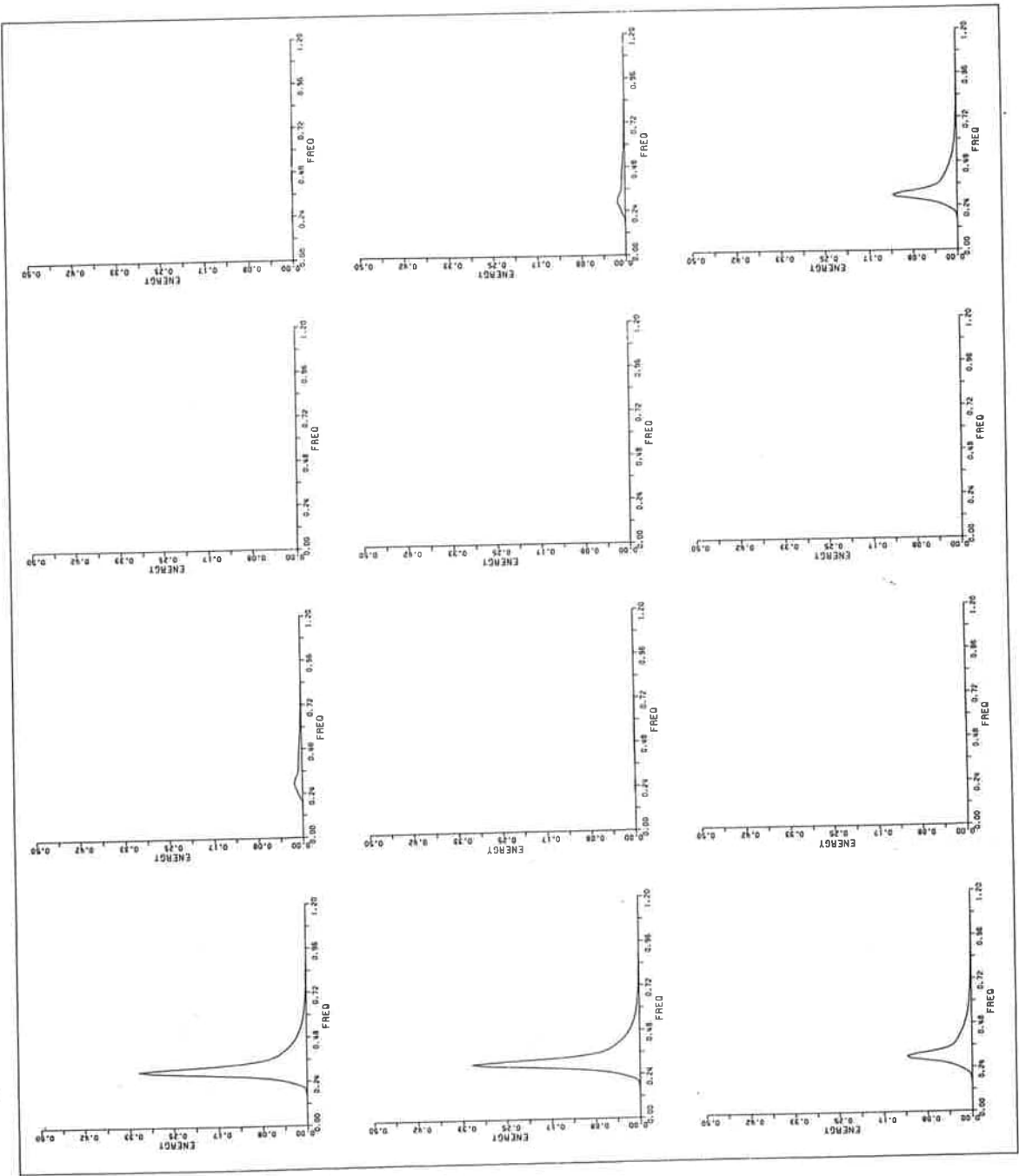


Fig. 2a  $E(f, \theta)$ :  $f_{1m} = 0.3\text{Hz}$ ,  $\theta_{1m} = 0^\circ$ ,  $f_{2m} = 0.3\text{Hz}$ ,  $\theta_{2m} = 30^\circ$

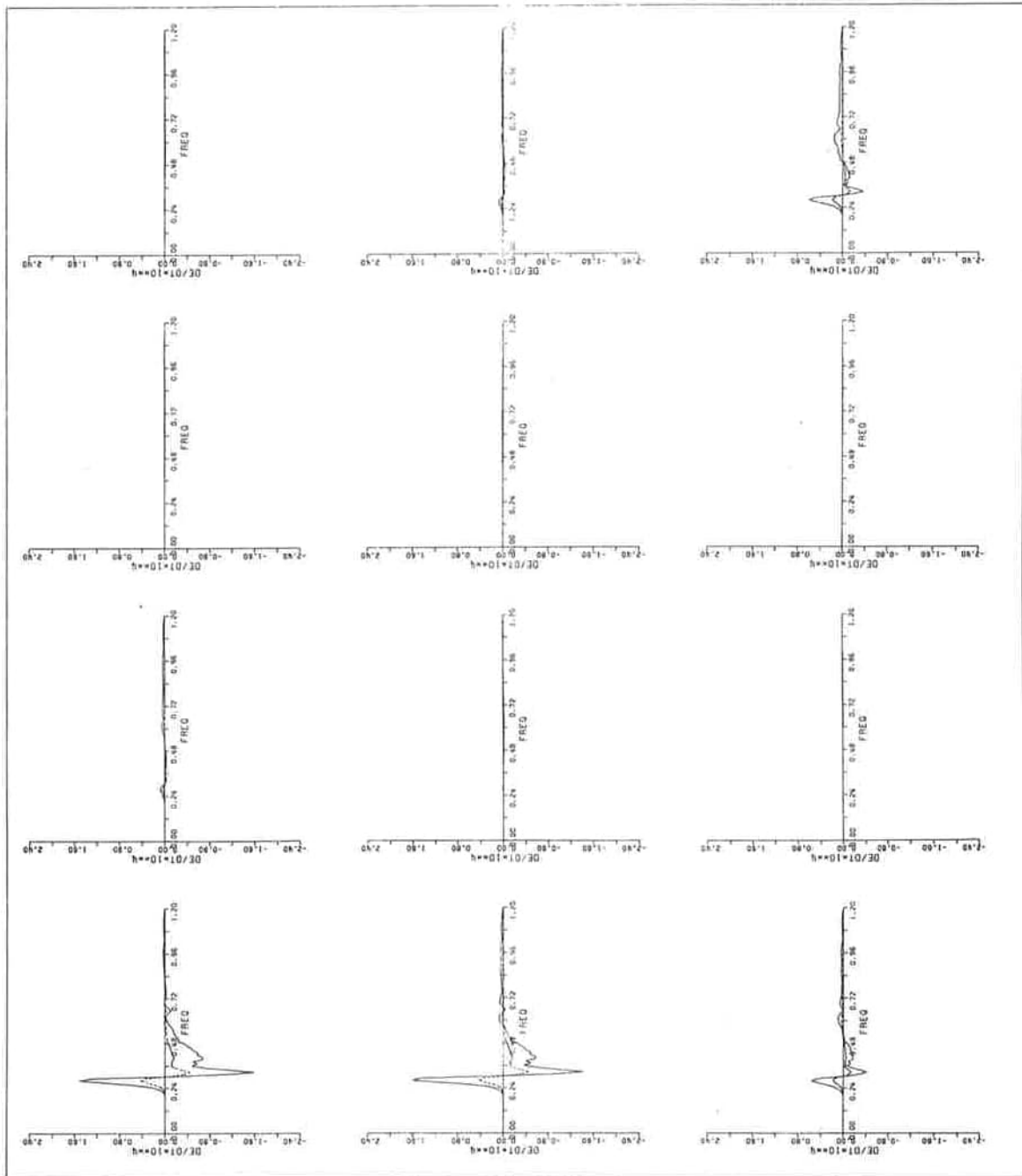


Fig. 2b  $S_{n1}(f, \theta)$

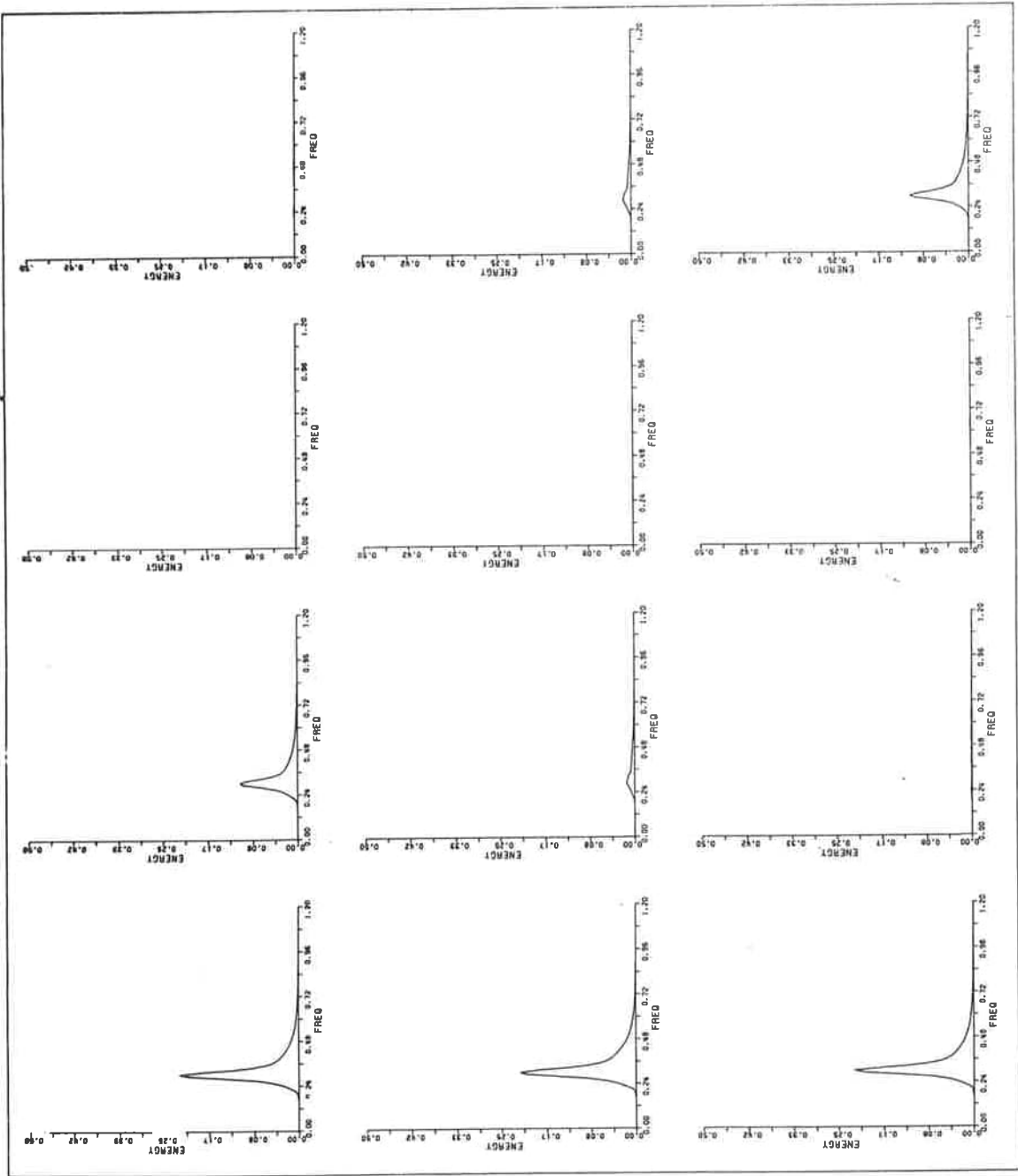


Fig. 3a  $E(f, \theta)$ :  $f_{\perp m} = 0.3\text{Hz}$ ,  $\theta_1 = 0^\circ$ ,  $f_{2m} = 0.3\text{Hz}$ ,  $\theta_{2m} = 0^\circ$

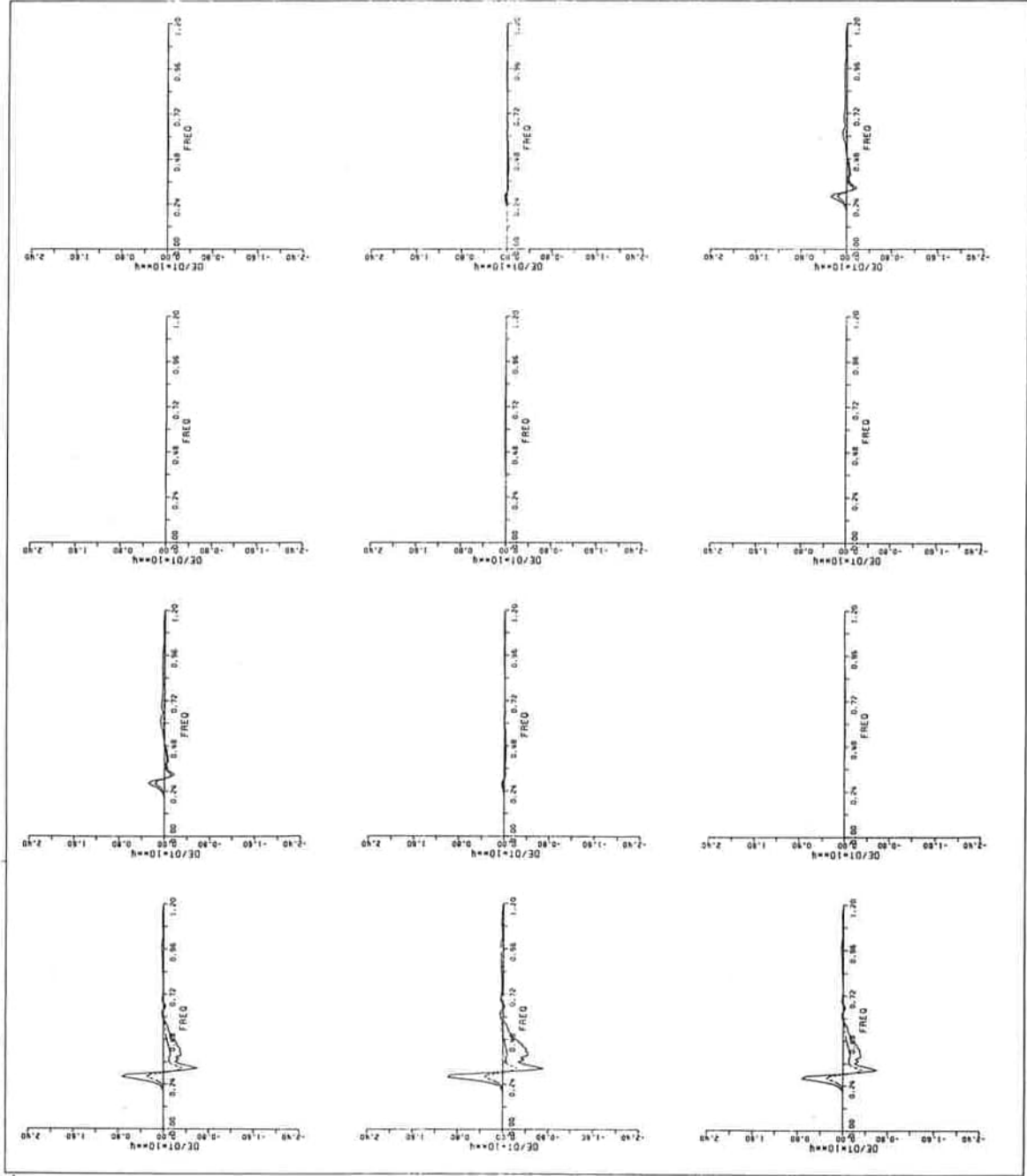


Fig. 3b  $S_{n1}(f, \theta)$

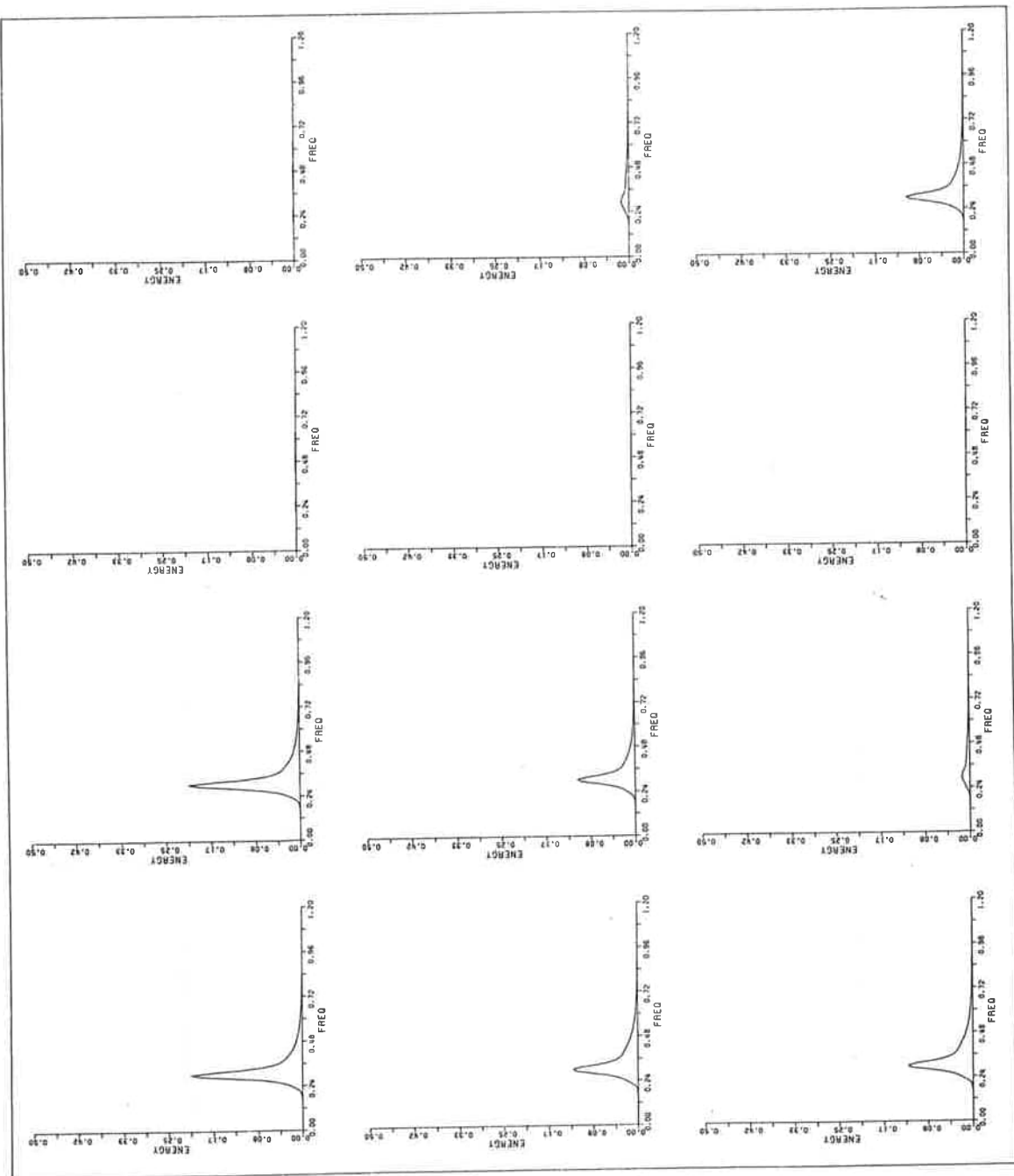


Fig. 4a  $E(\epsilon, \theta)$ :  $f_{1m} = 0.3\text{Hz}$ ,  $\theta_{1m} = 0^\circ$ ,  $f_{2m} = 0.3\text{Hz}$ ,  $\theta_{2m} = 90^\circ$

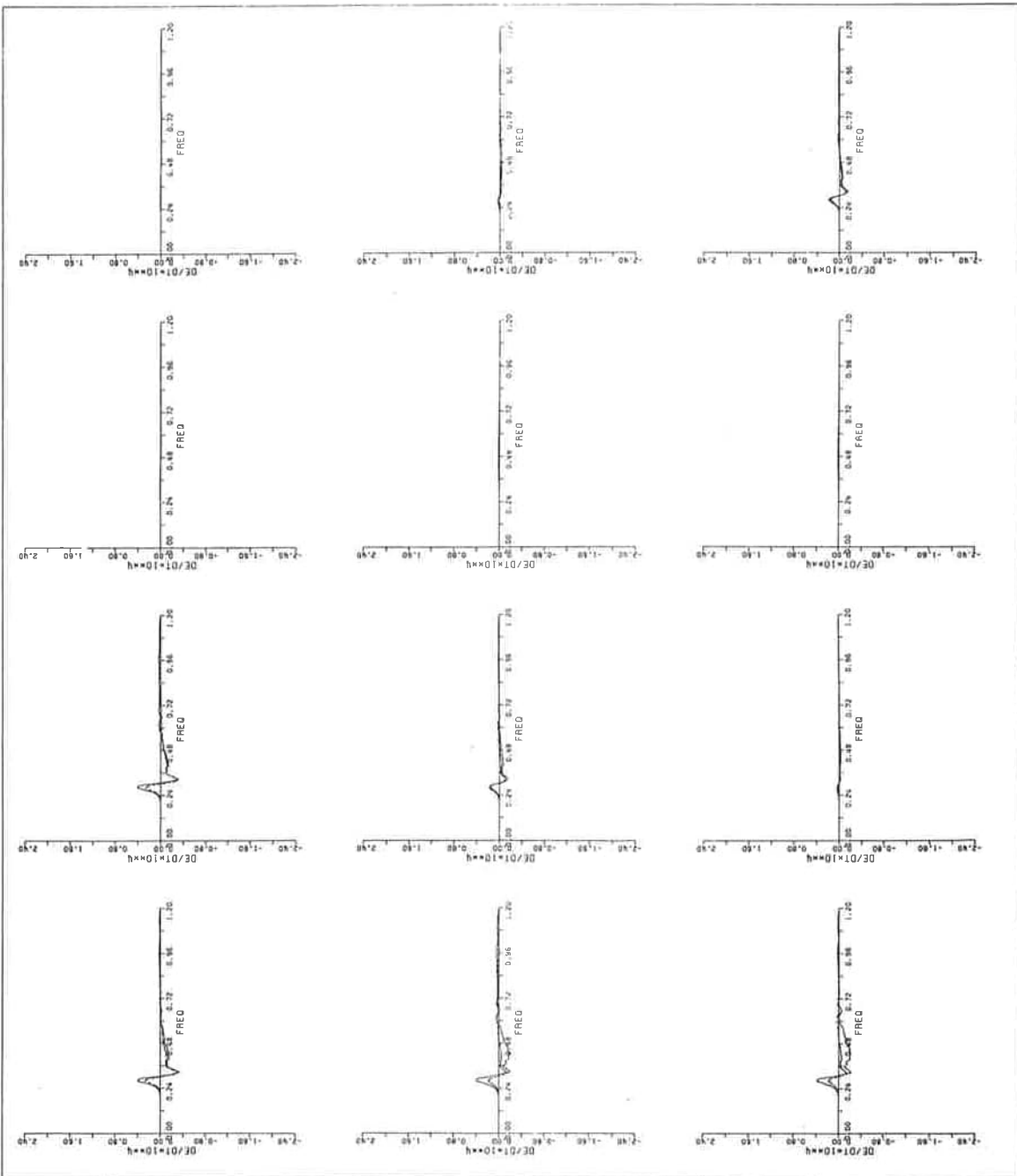


Fig. 4b  $S_{n1}(f, \theta)$

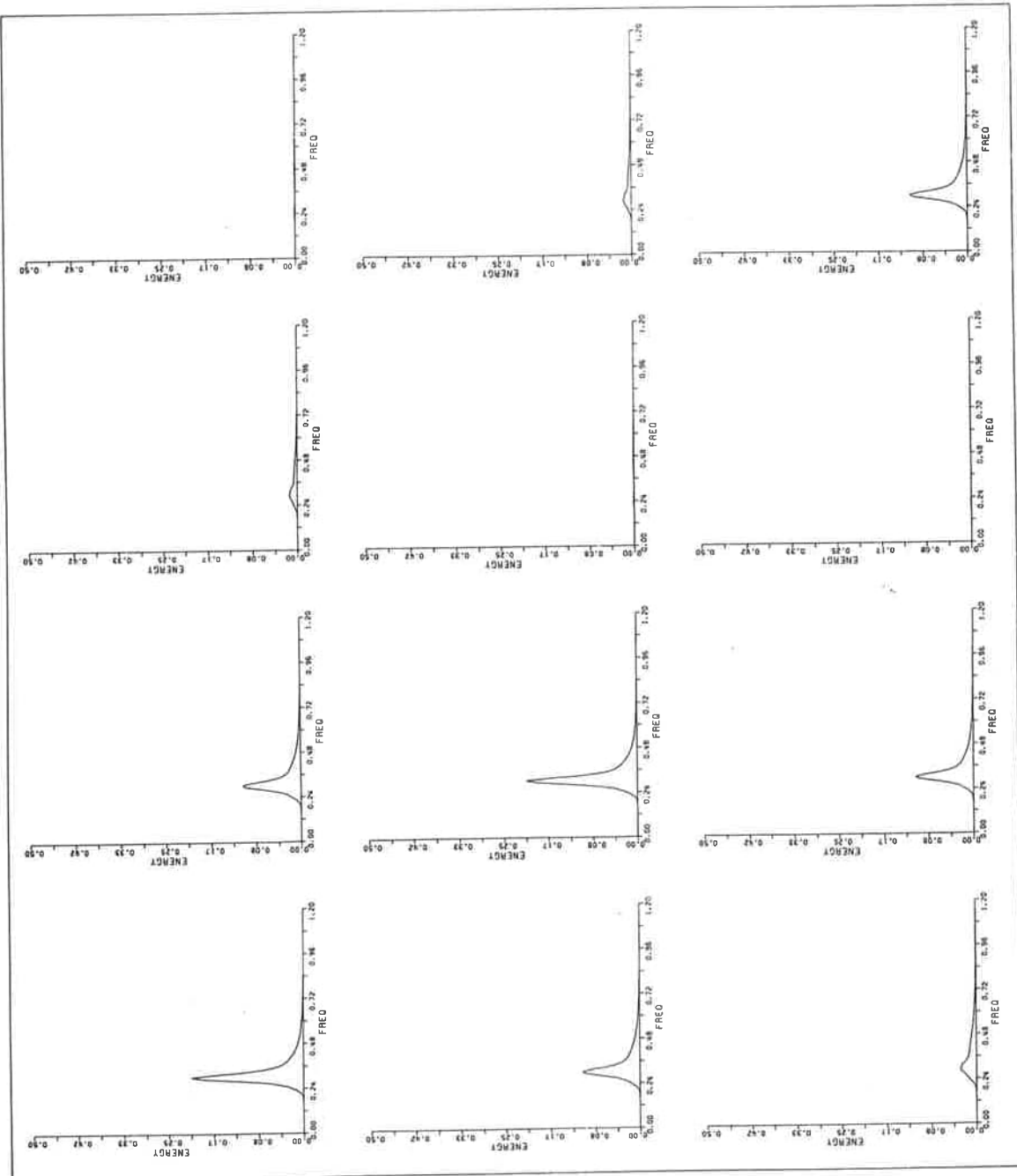
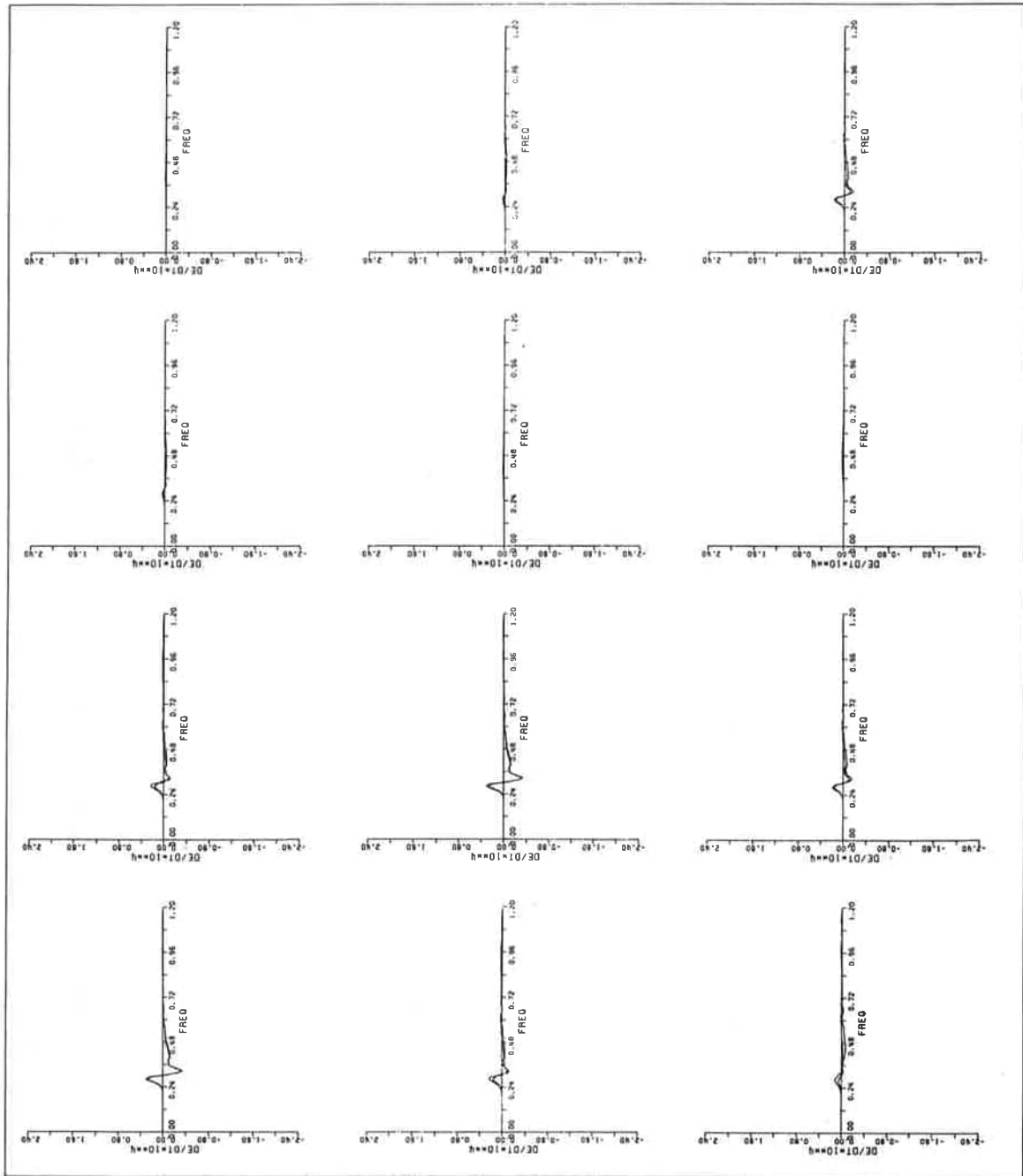


Fig. 5a  $E(f, \theta)$ :  $f_{1m} = 0.3\text{Hz}$ ,  $\theta_{1m} = 0^\circ$ ,  $f_{2m} = 0.3\text{Hz}$ ,  $\theta_{2m} = 120^\circ$

Fig. 5b  $S_{nl}(f, \theta)$



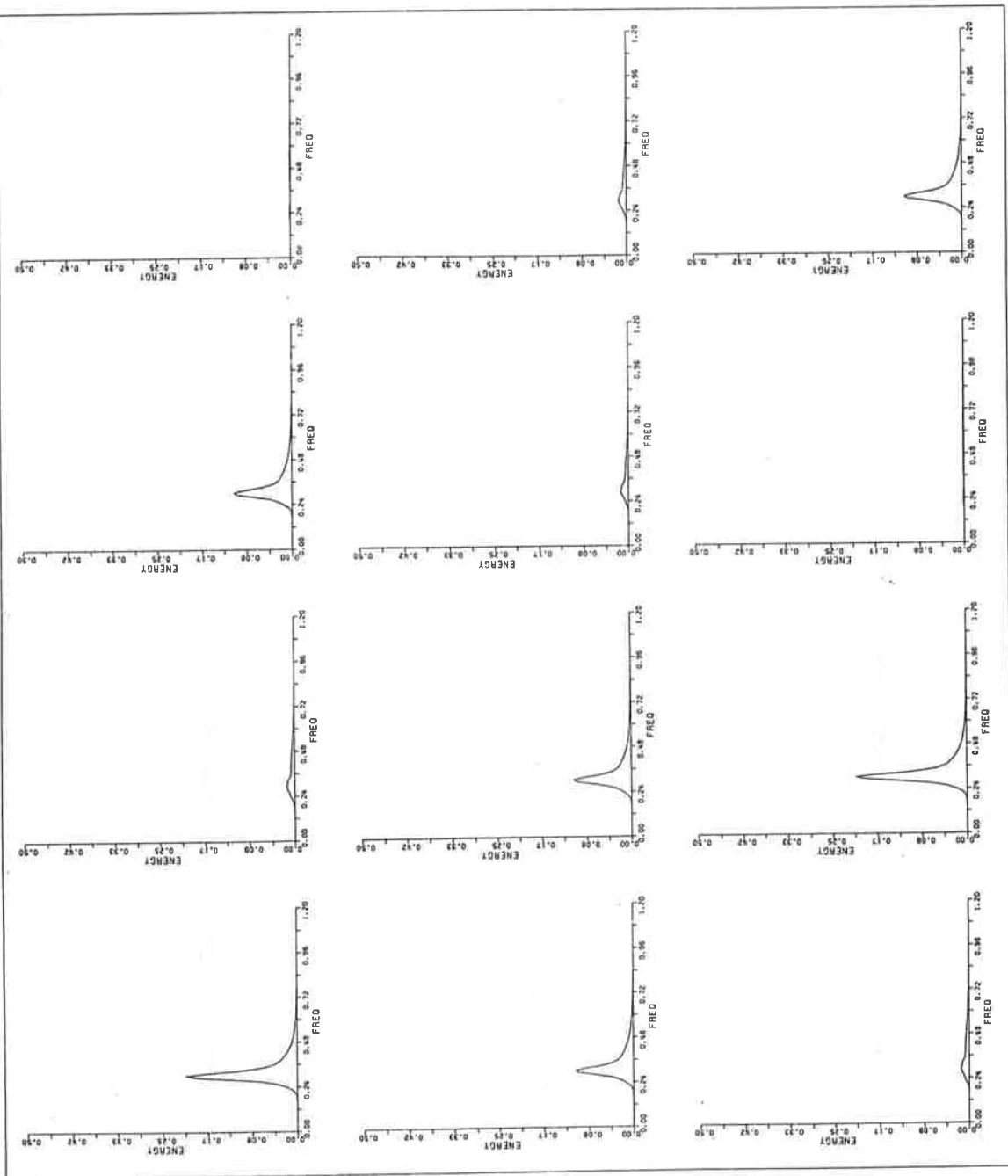
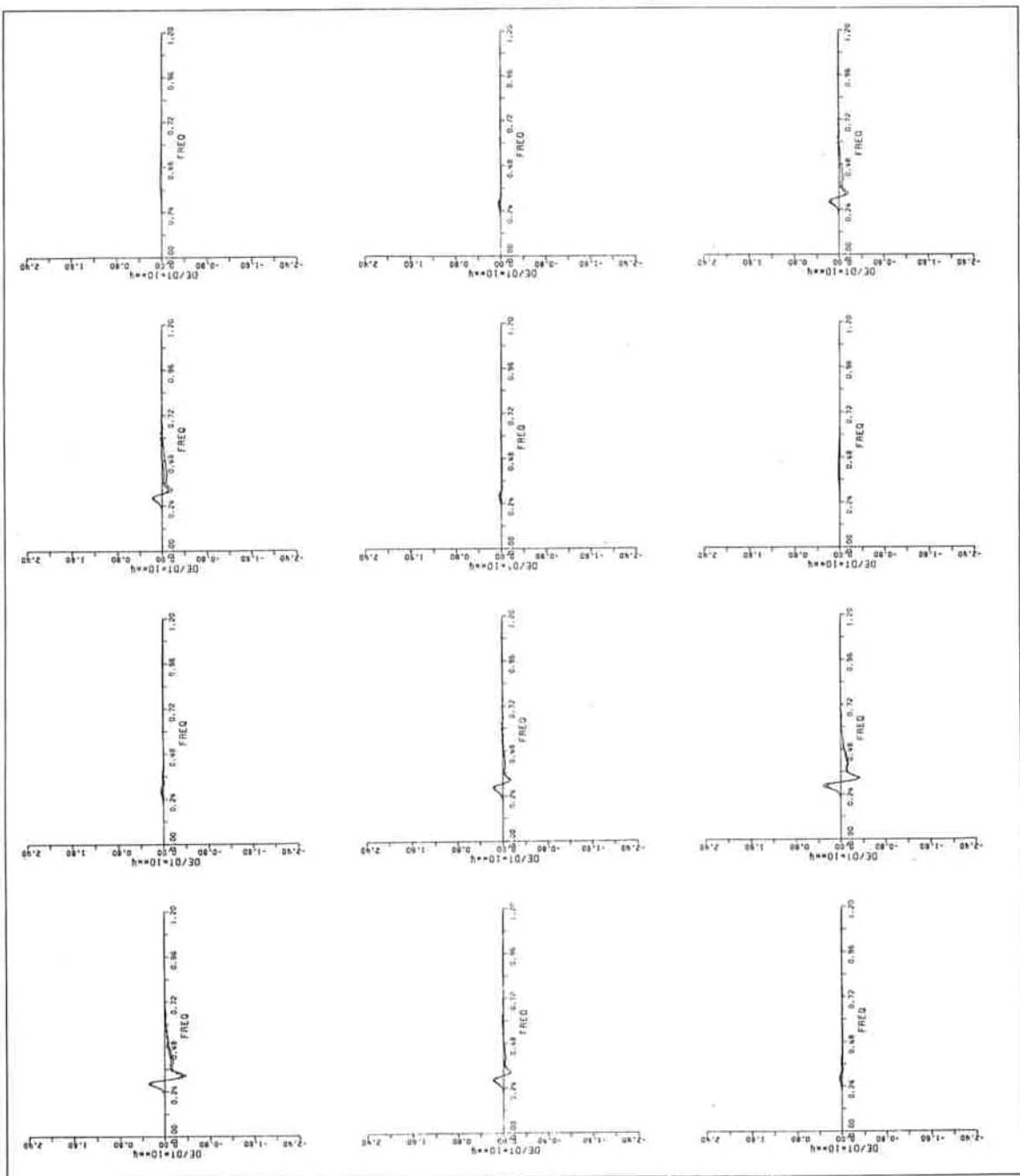


Fig. 6a  $E(f, \theta)$ :  $f_{1m} = 0.3\text{Hz}$ ,  $\theta_{1m} = 0^\circ$ ,  $f_{2m} = 0.3\text{Hz}$ ,  $\theta_{2m} = 150^\circ$

Fig. 6b  $S_{n1}(\mathbf{f}, \theta)$



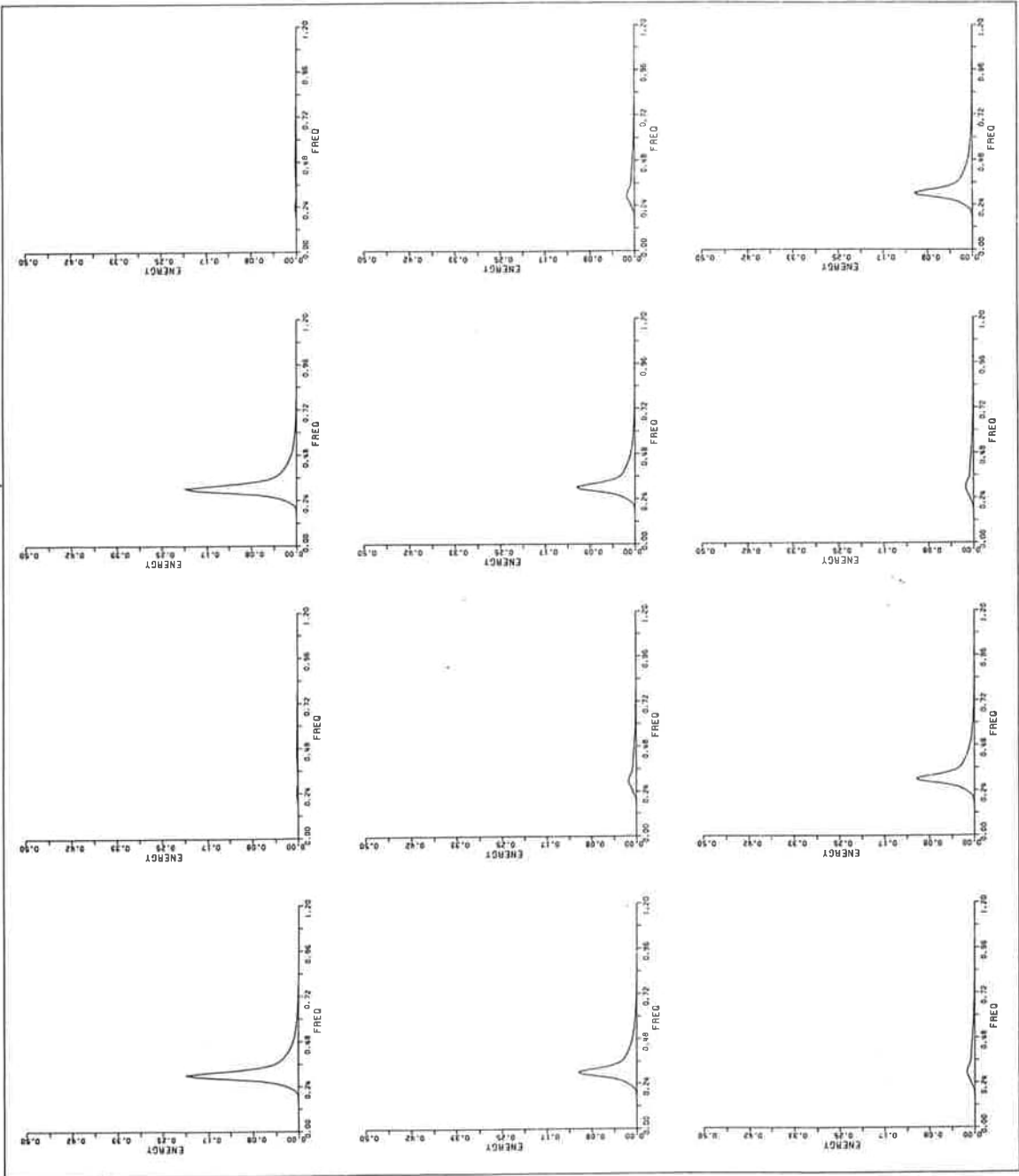


Fig. 7a  $E(f, \theta)$ :  $f_{1m} = 0.3\text{Hz}$ ,  $\theta_{1m} = 0^\circ$ ,  $f_{2m} = 0.3\text{Hz}$ ,  $\theta_{2m} = 180^\circ$

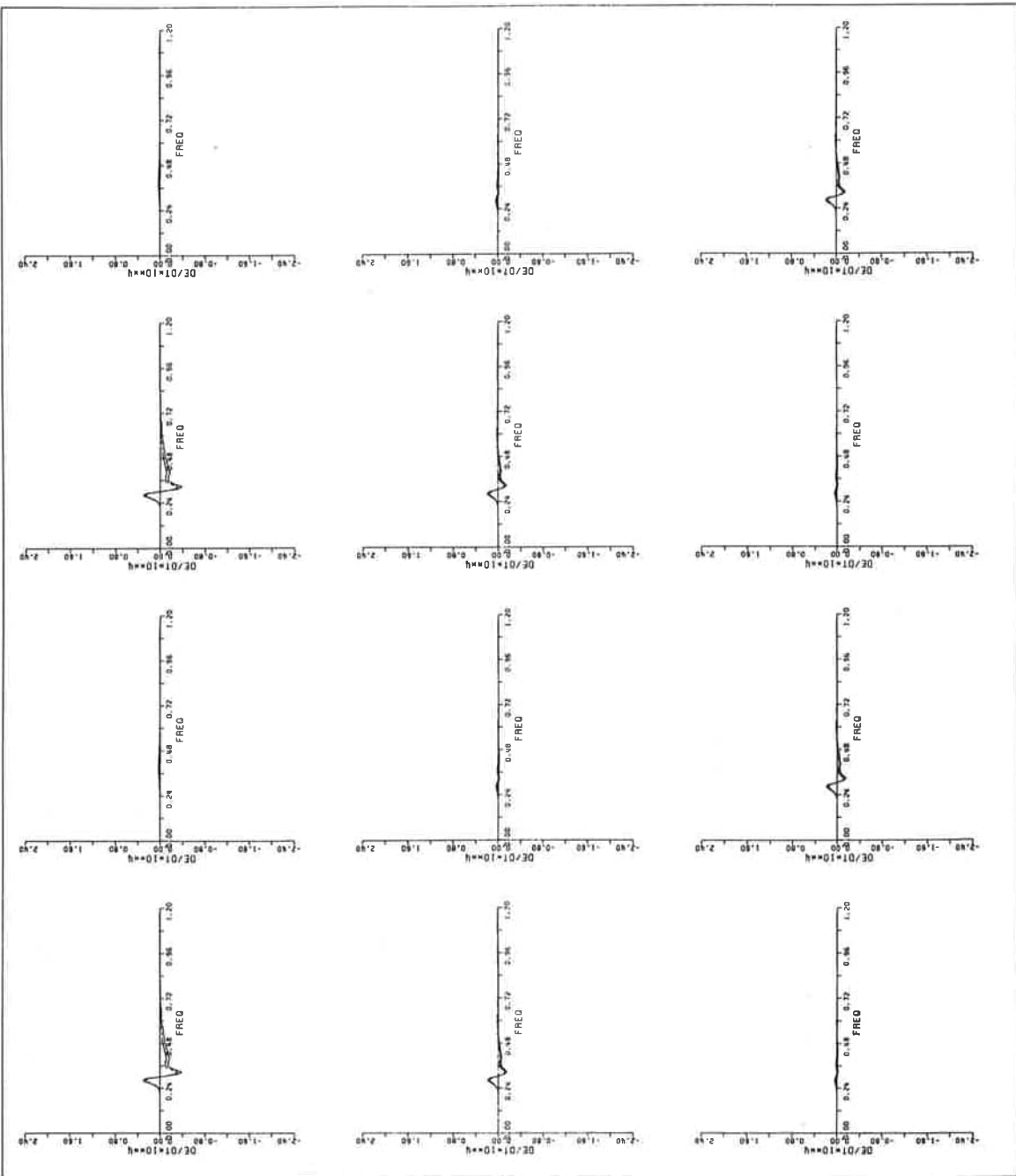


Fig. 7b  $S_{n1}(f, \theta)$

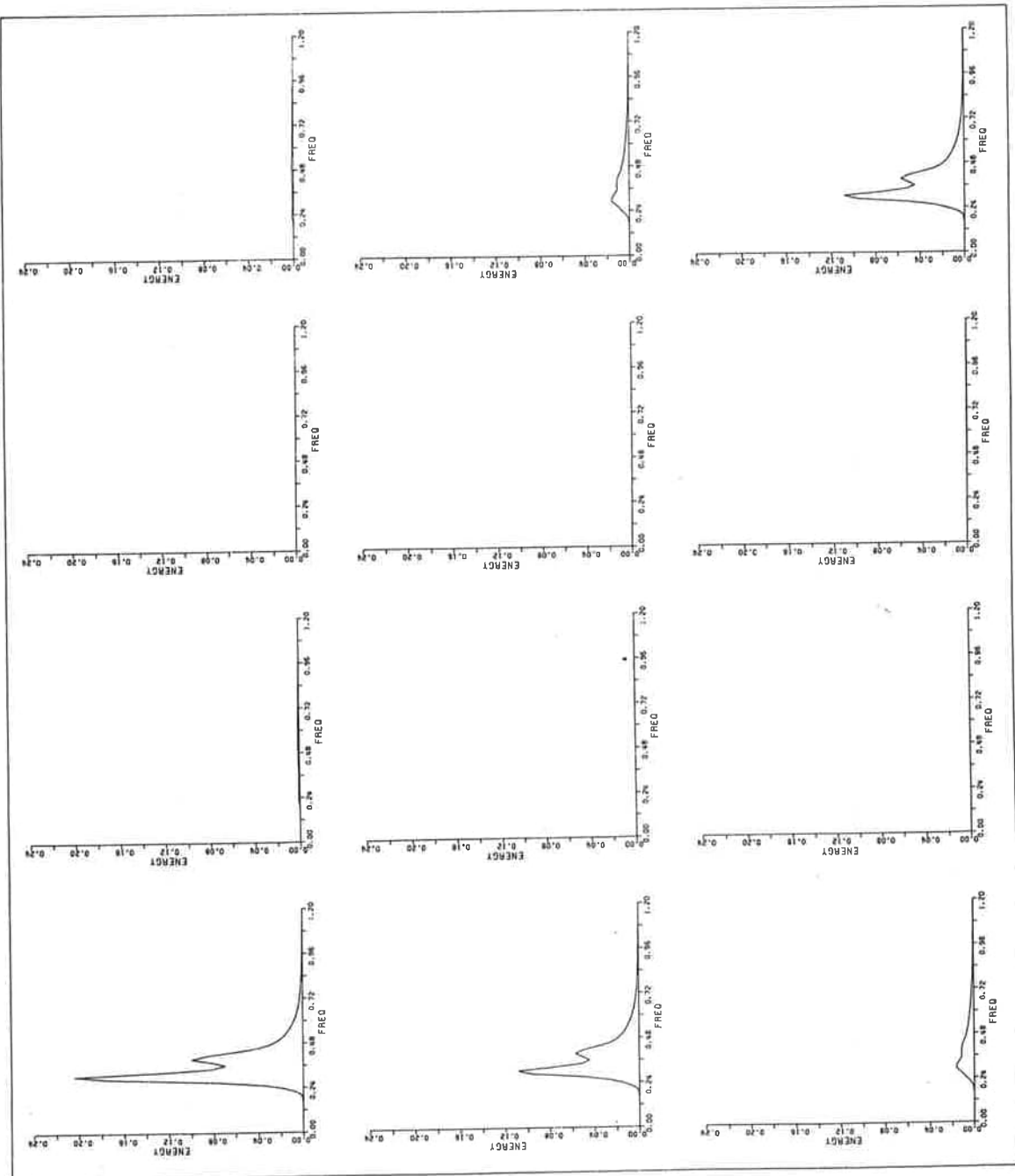


Fig. 8a  $E(f, \theta)$ :  $f_{1m} = 0.3\text{Hz}$ ,  $\theta_{1m} = 0^\circ$ ,  $f_{2m} = 0.4\text{Hz}$ ,  $\theta_{2m} = 0^\circ$

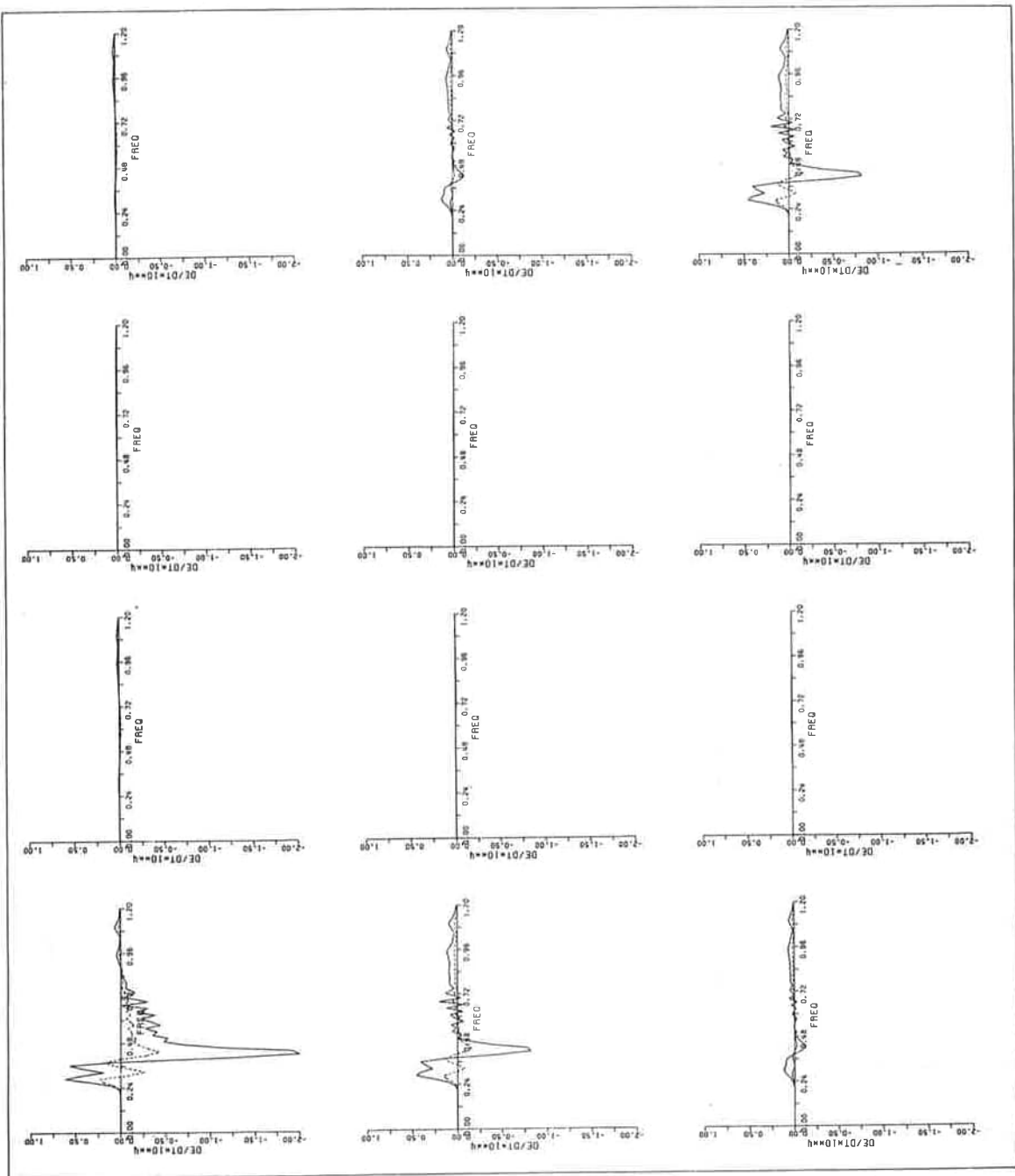


Fig. 8b  $S_{nl}(f, \theta)$

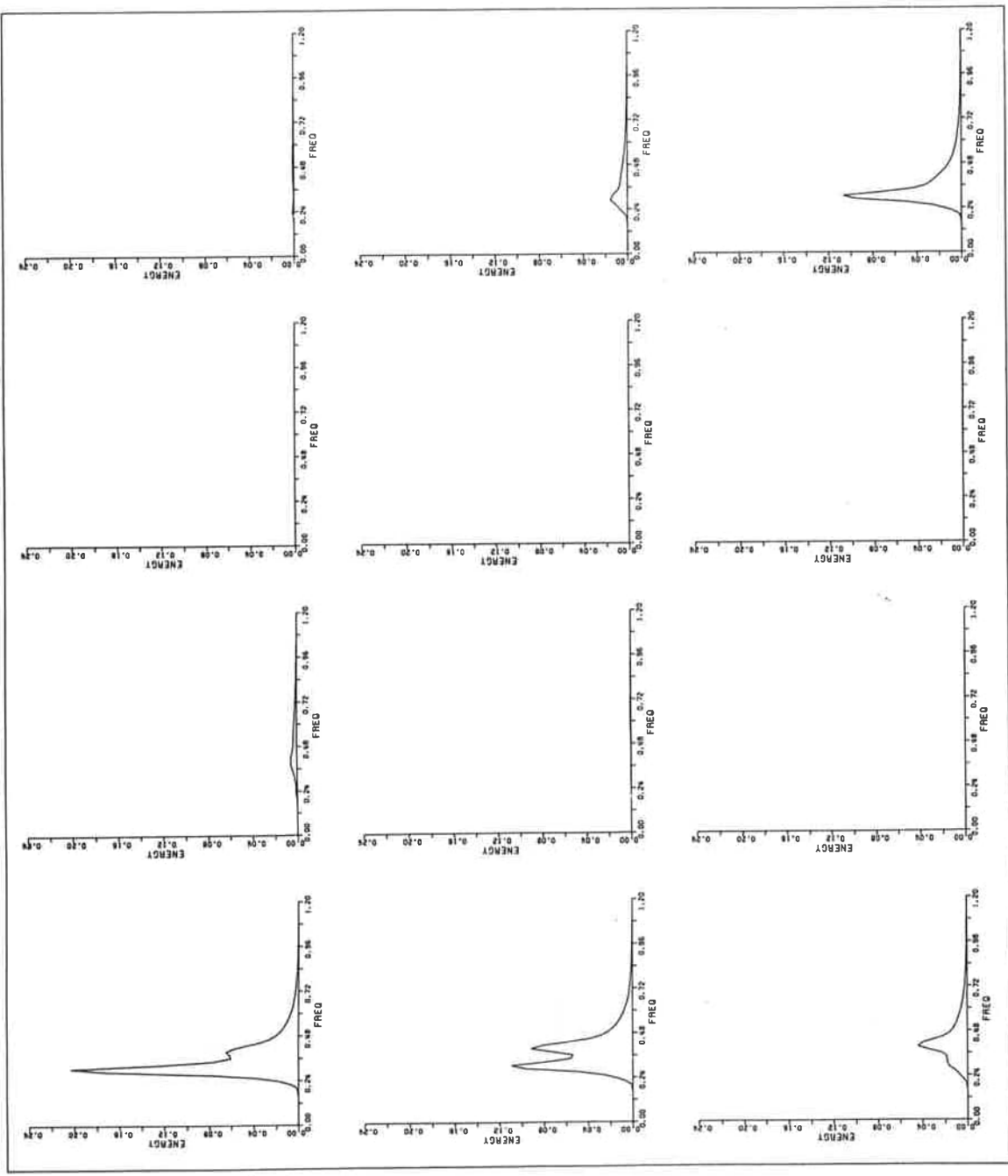
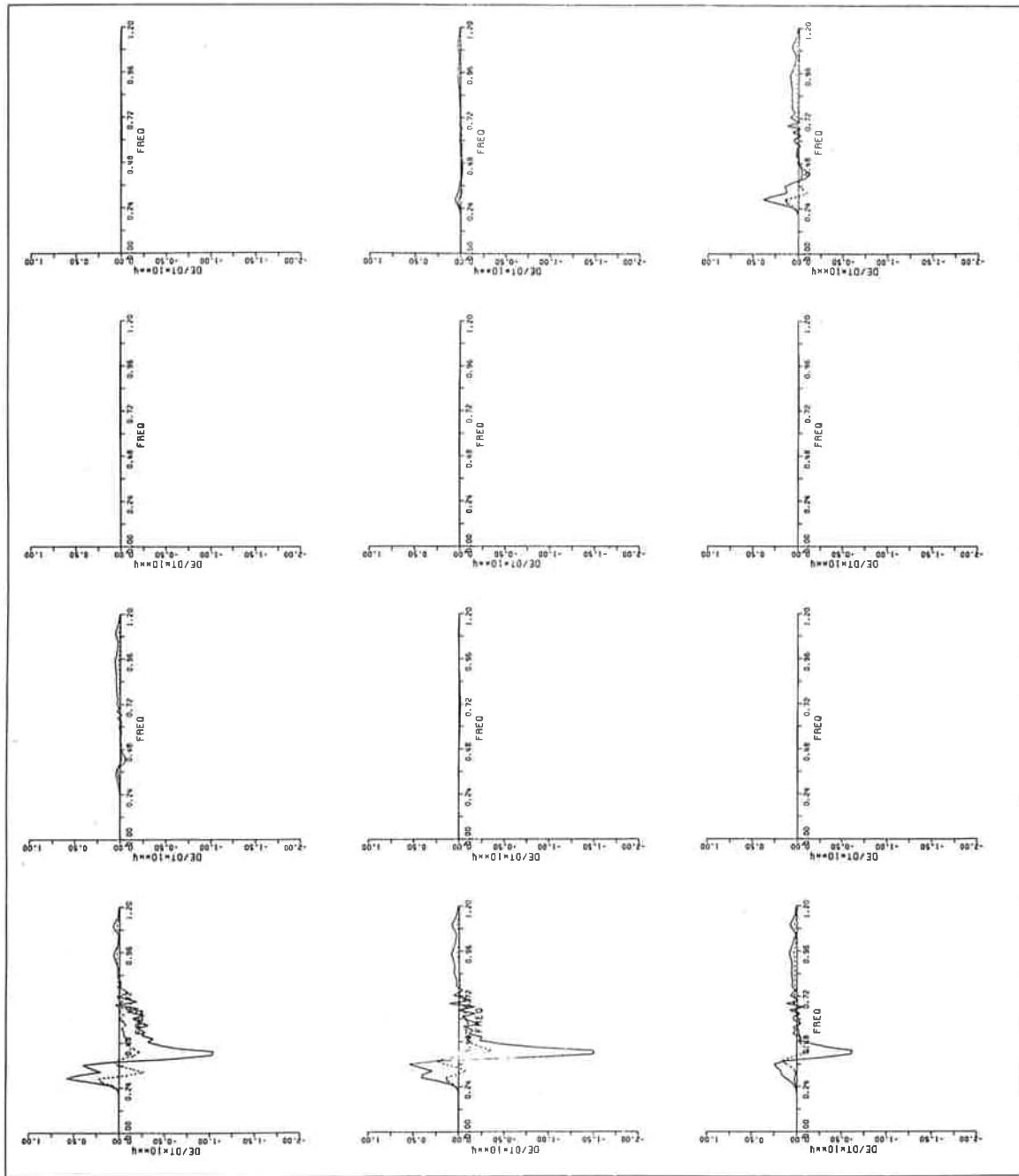


Fig. 9a  $E(f, \theta)$ :  $f_{1m} = 0.3\text{Hz}$ ,  $\theta_{1m} = 0^\circ$ ,  $f_{2m} = 0.4\text{Hz}$ ,  $\theta_{2m} = 30^\circ$

Fig. 9b  $S_{n1}(f, \theta)$



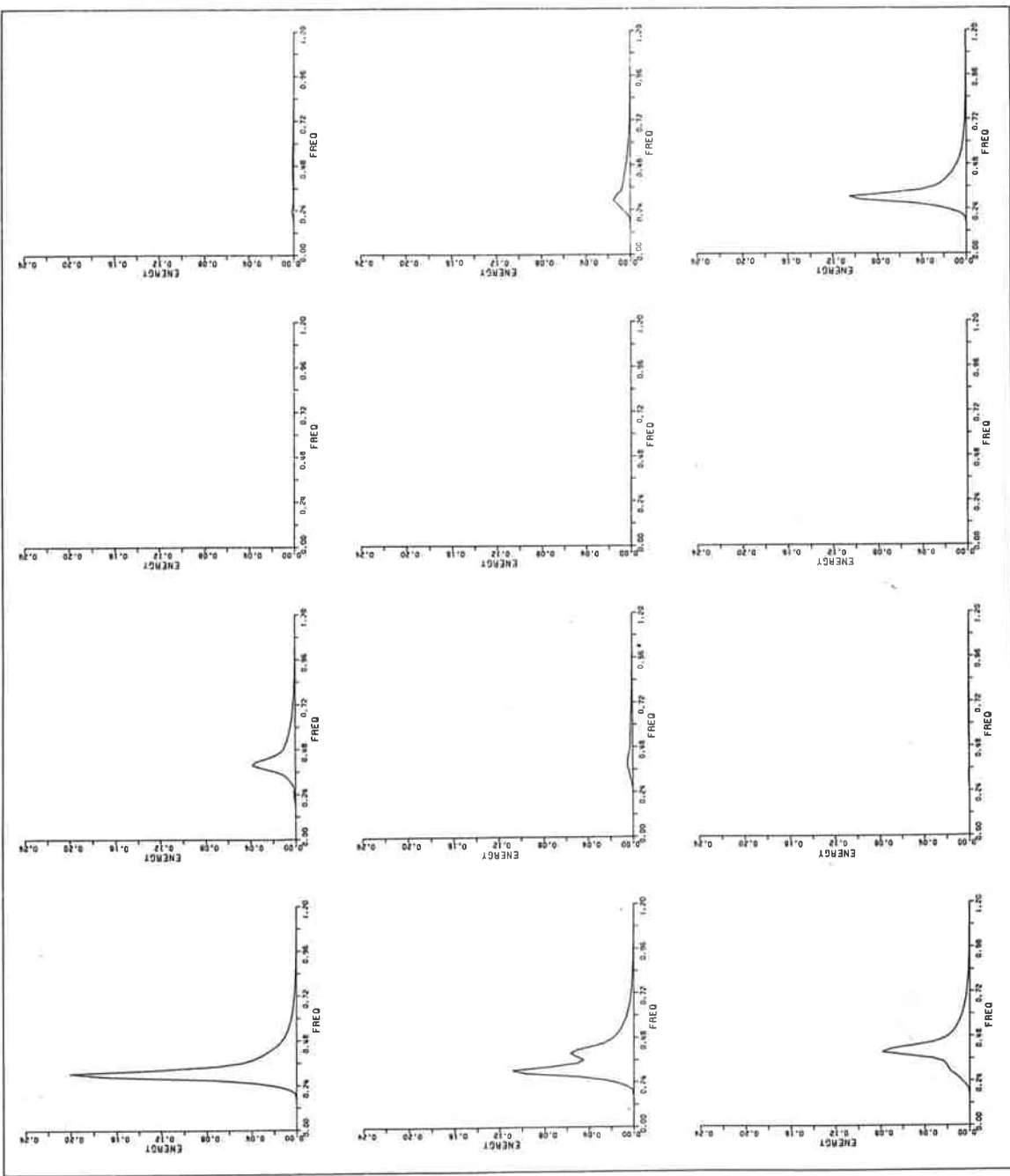
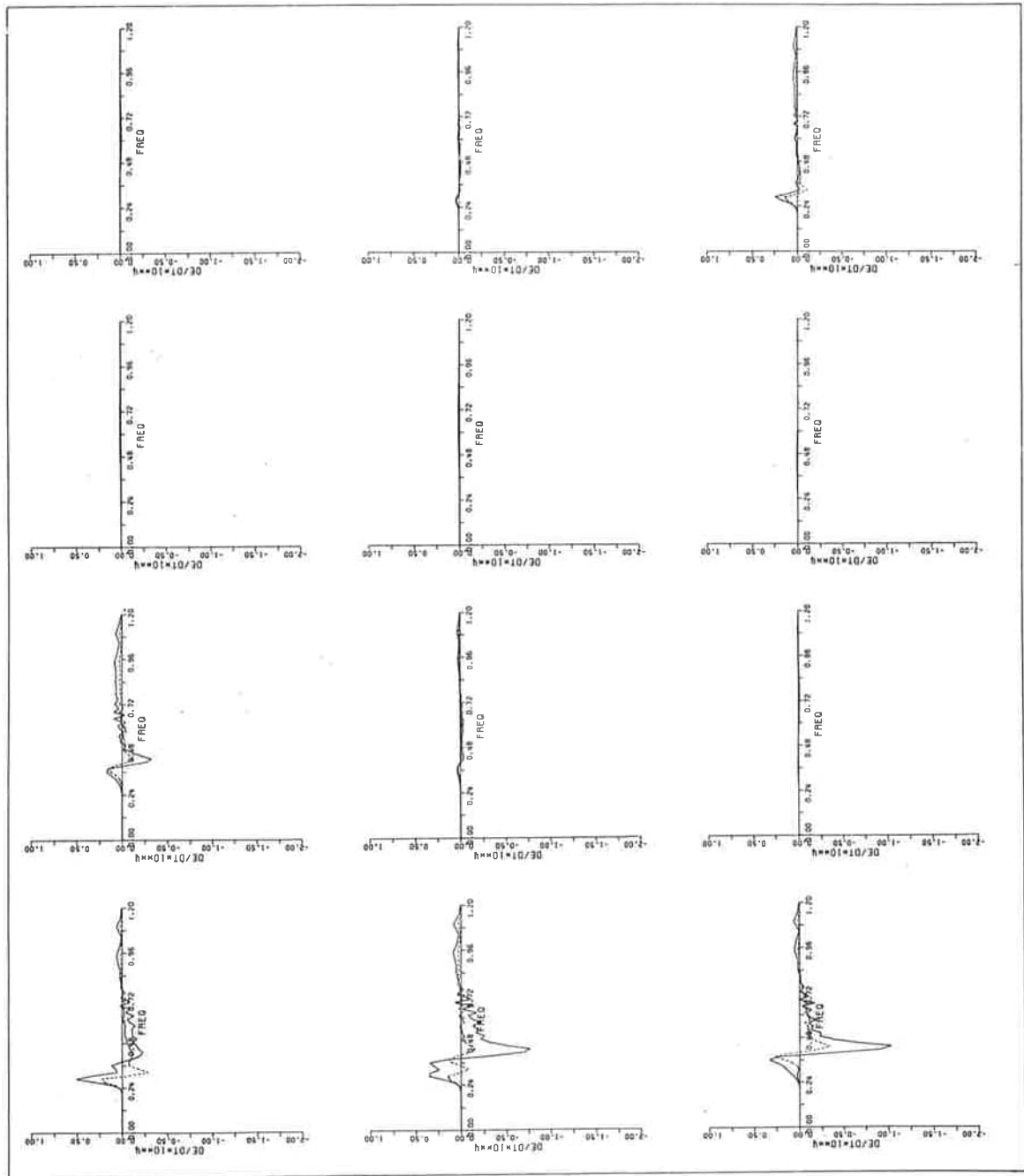


Fig. 10a  $E(f, \theta)$ :  $f_{1m} = 0.3\text{Hz}$ ,  $\theta_{1m} = 0^\circ$ ,  $f_{2m} = 0.4\text{Hz}$ ,  $\theta_{2m} = 60^\circ$

Fig. 10b  $S_{n1}(f, \theta)$



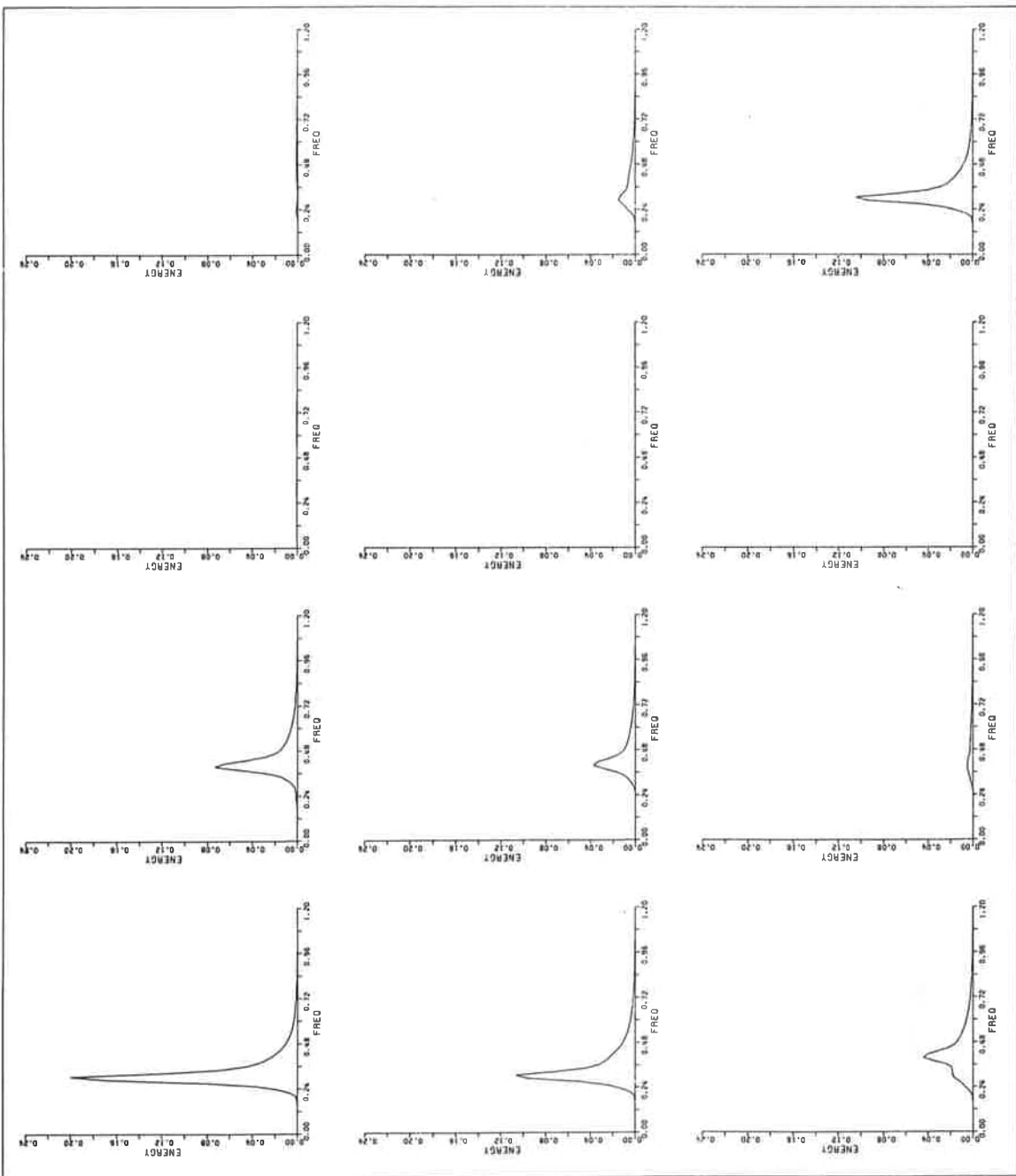


Fig. 11a  $E(f, \theta)$ :  $f_{1m} = 0.3\text{Hz}$ ,  $\theta_{1m} = 0^\circ$ ,  $f_{2m} = 0.4\text{Hz}$ ,  $\theta_{2m} = 90^\circ$

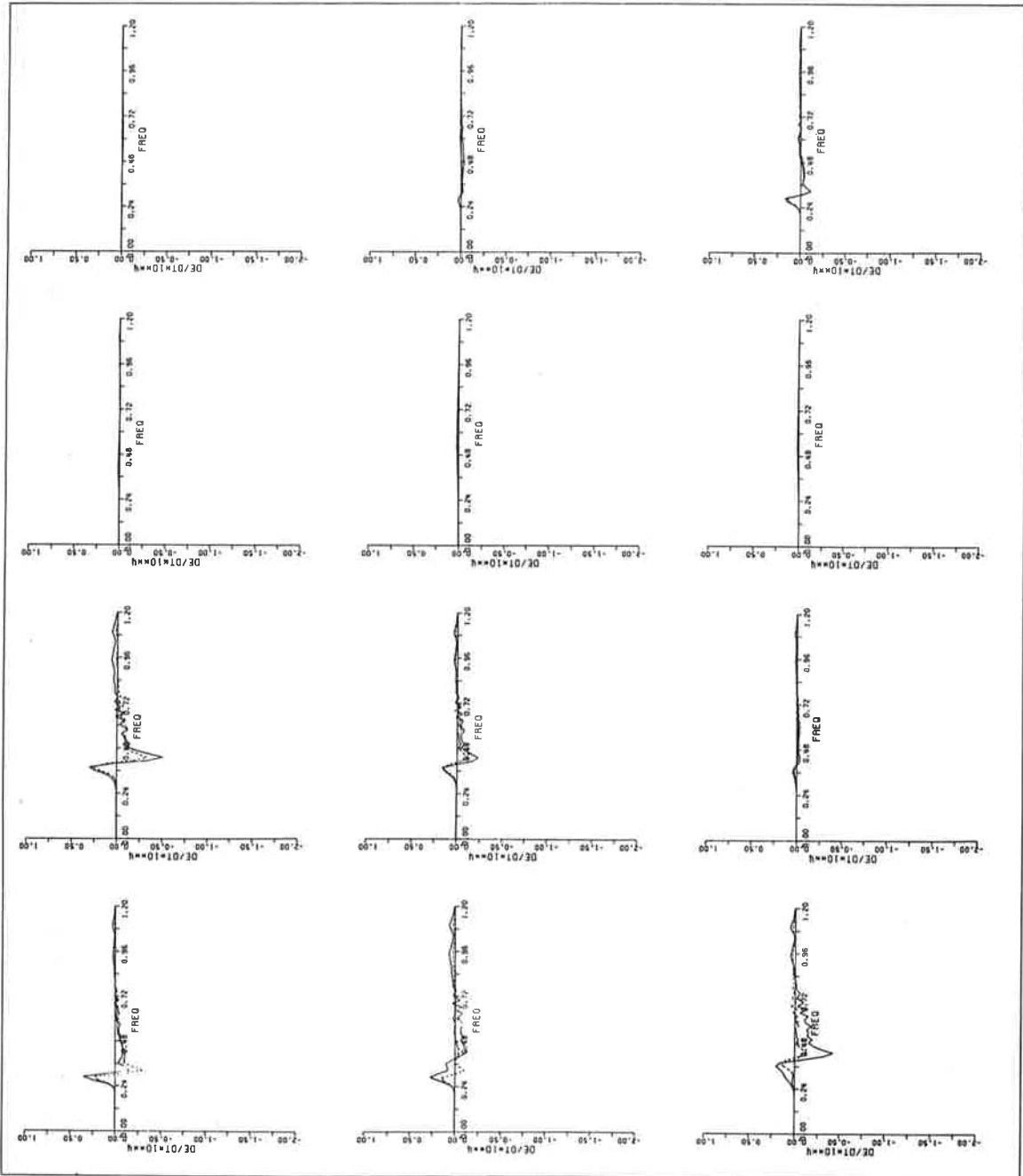


Fig. 11b  $S_{nl}(f, \theta)$

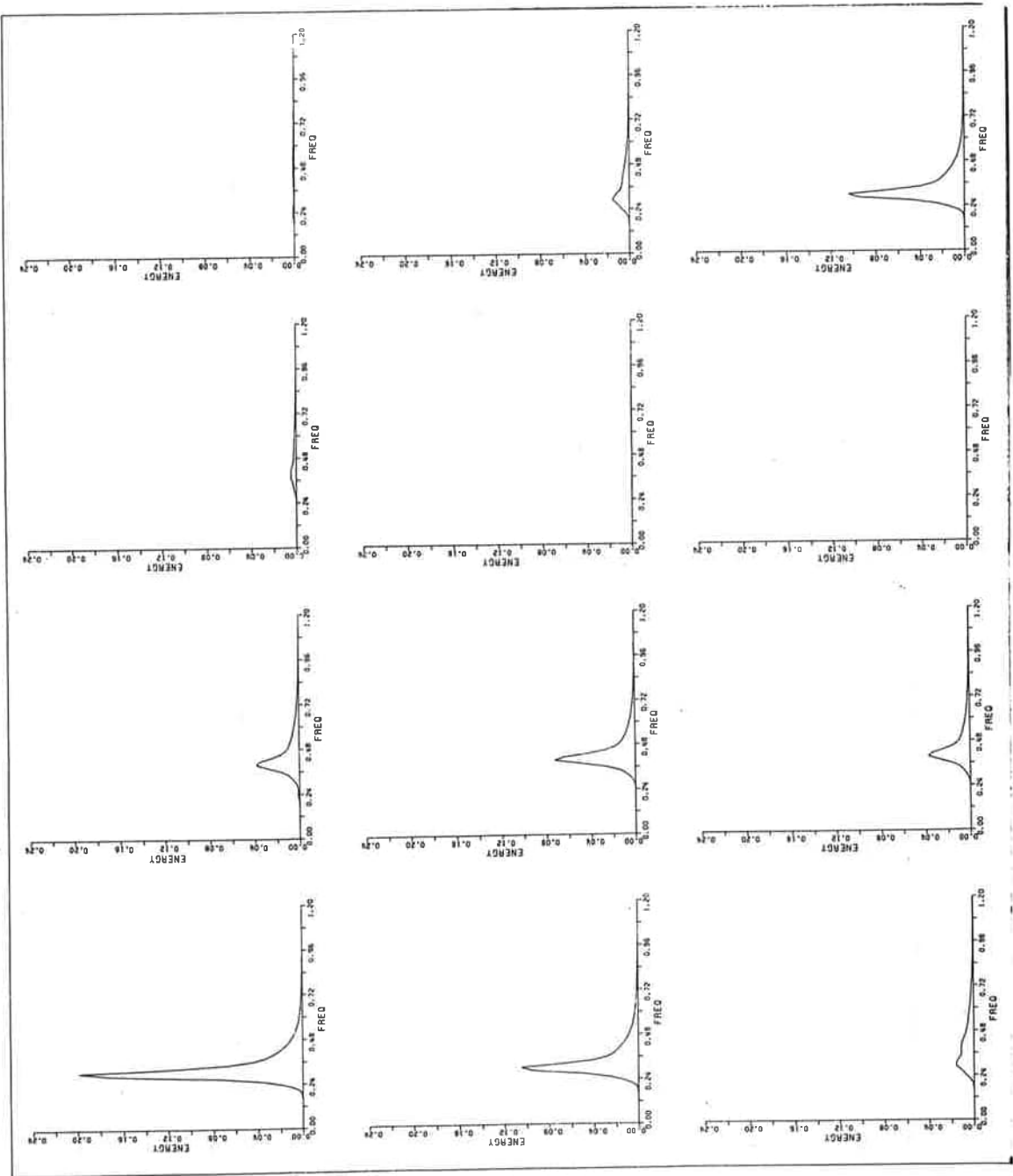


Fig. 12a  $E(f, \theta)$ :  $f_{1m} = 0.3\text{Hz}$ ,  $\theta_{1m} = 0^\circ$ ,  $f_{2m} = 0.4\text{Hz}$ ,  $\theta_{2m} = 120^\circ$

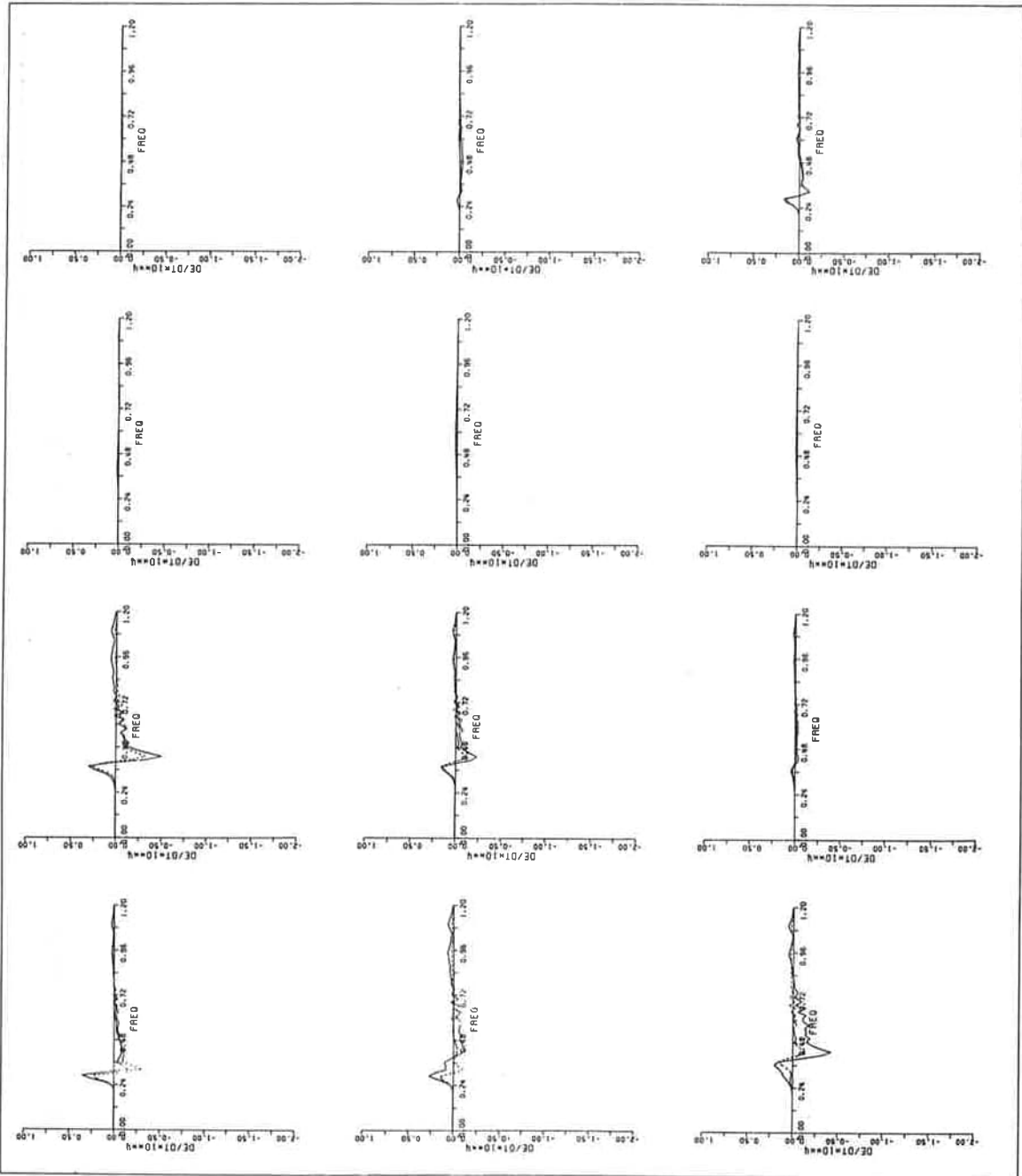


Fig. 11b  $S_{n1}(f, \theta)$

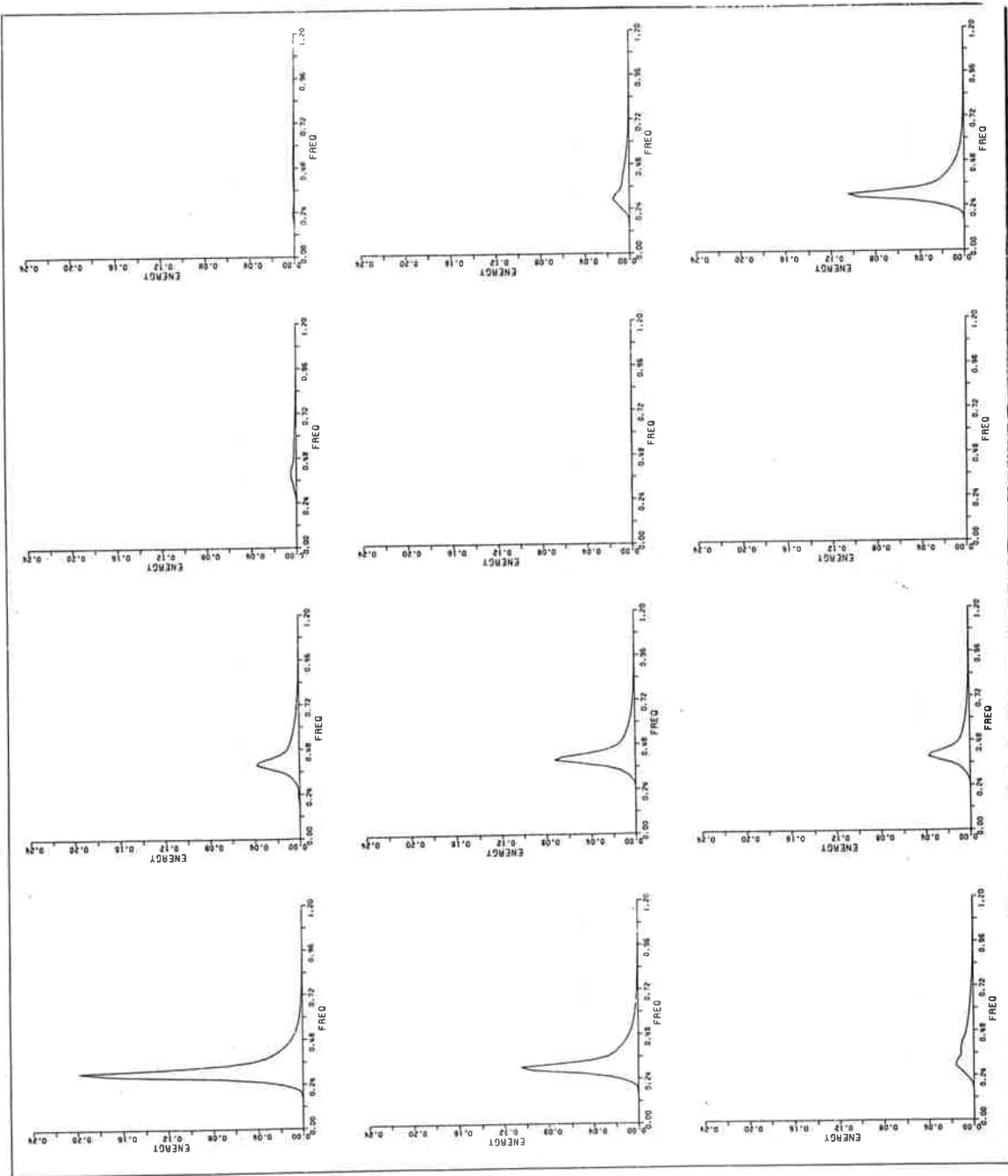


Fig. 12a  $E(f, \theta)$ :  $f_{1m} = 0.3\text{Hz}$ ,  $\theta_{1m} = 0^\circ$ ,  $f_{2m} = 0.4\text{Hz}$ ,  $\theta_{2m} = 120^\circ$

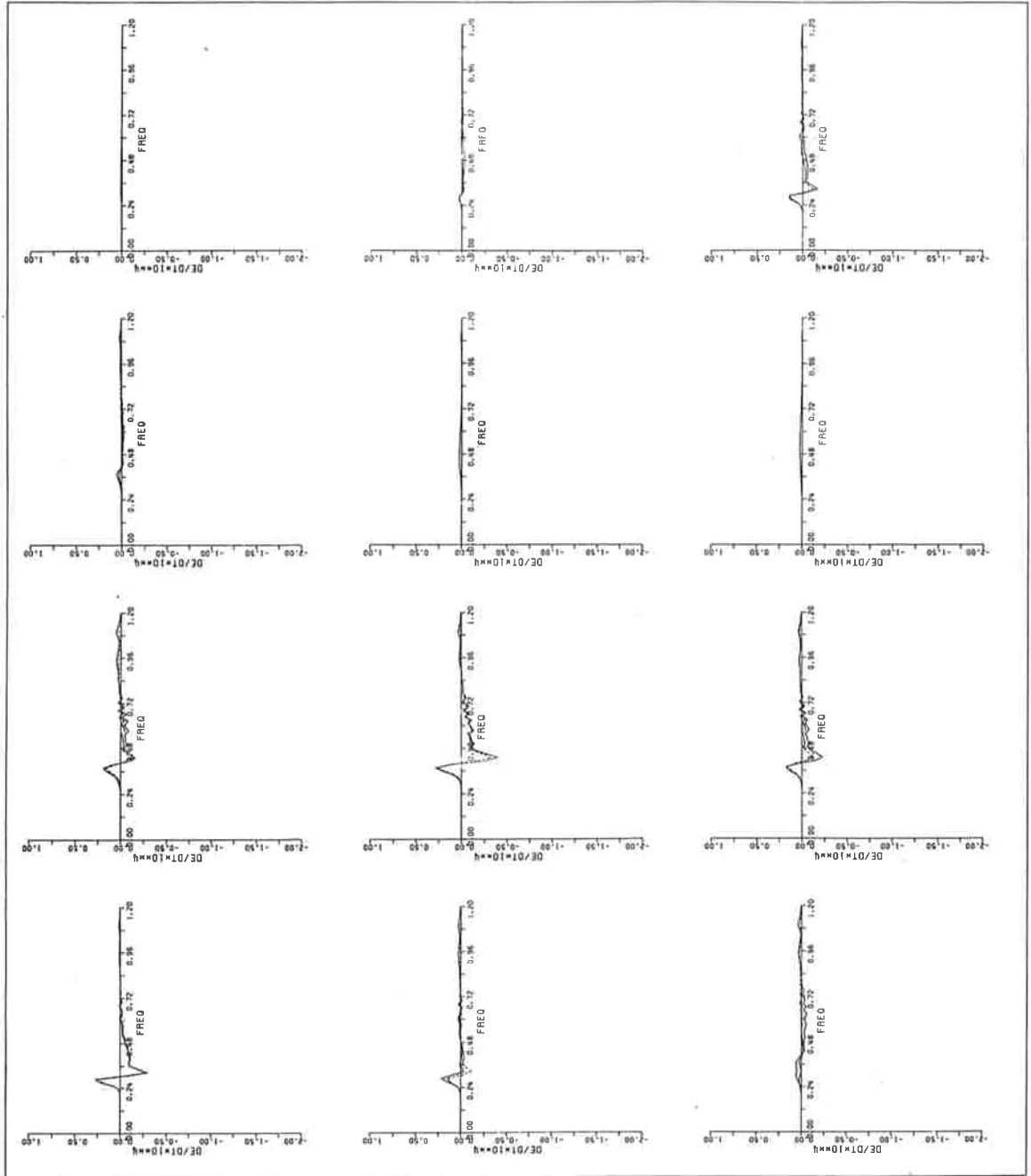


Fig. 112b  $S_{nl}(f, \theta)$

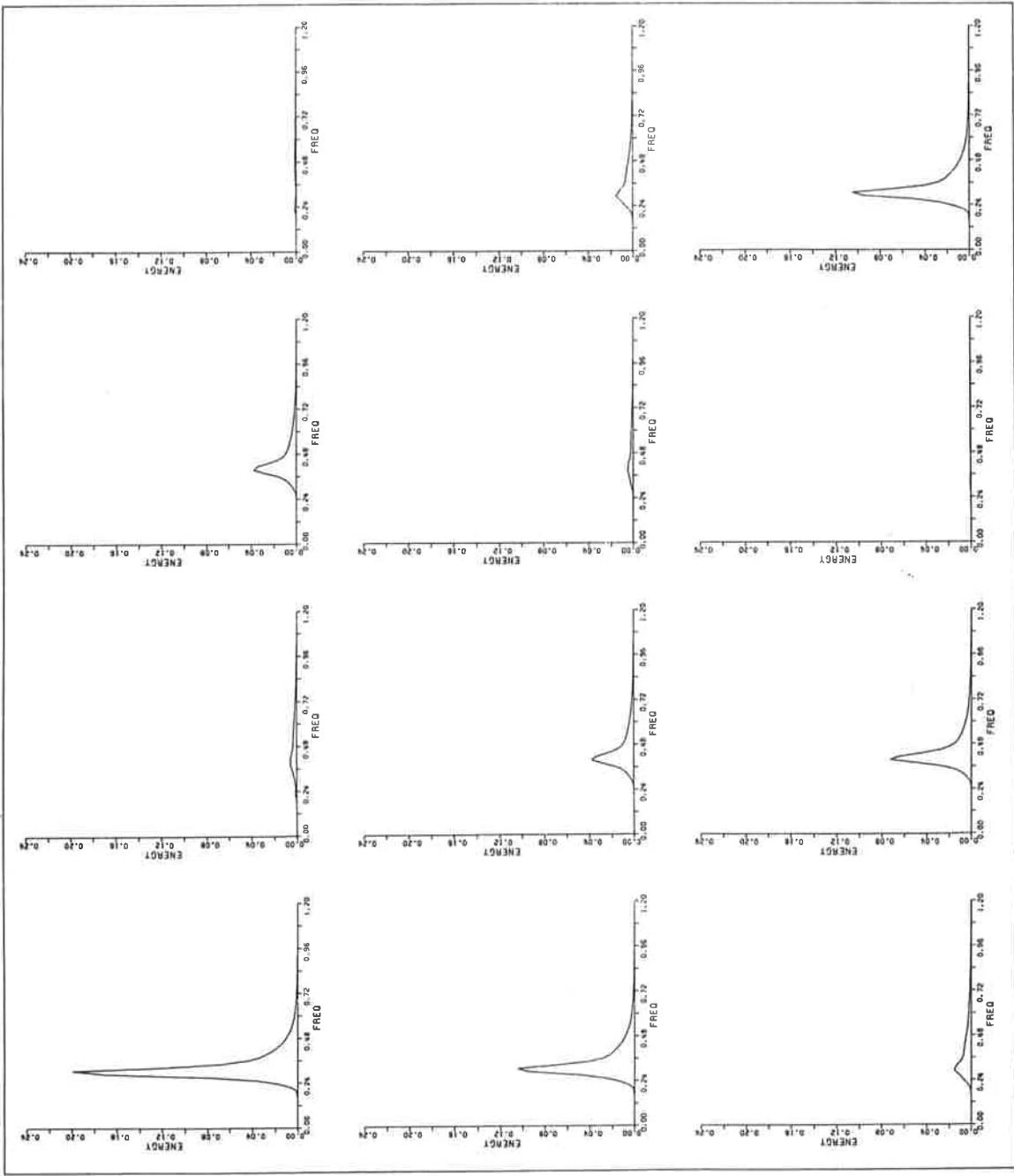


Fig. 13a  $E(f, \theta)$ :  $f_{1m} = 0.3\text{Hz}$ ,  $\theta_{1m} = 0^\circ$ ,  $f_{2m} = 0.4\text{Hz}$ ,  $\theta_{2m} = 150^\circ$

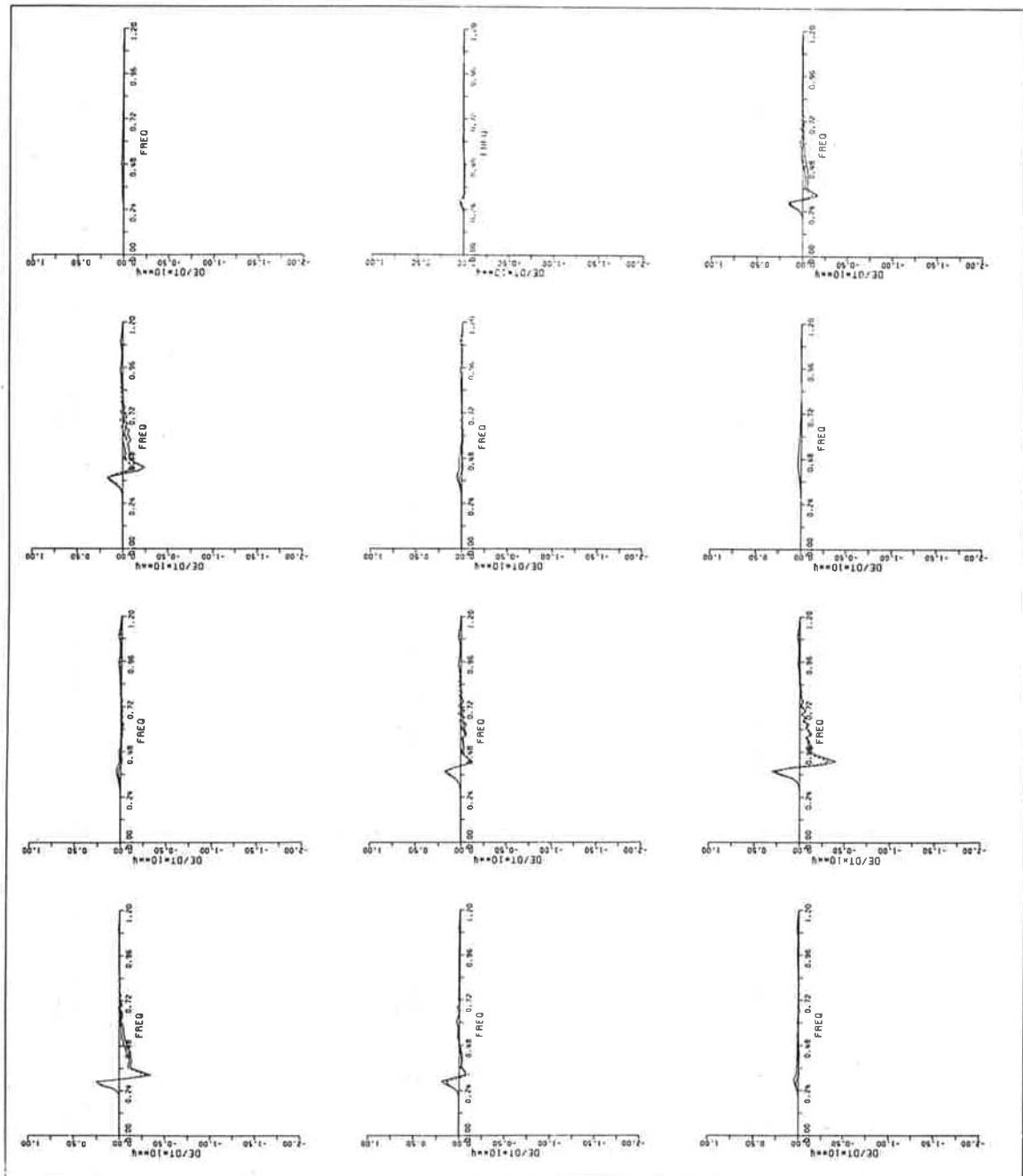


Fig. 13b  $S_{n1}(f, \theta)$

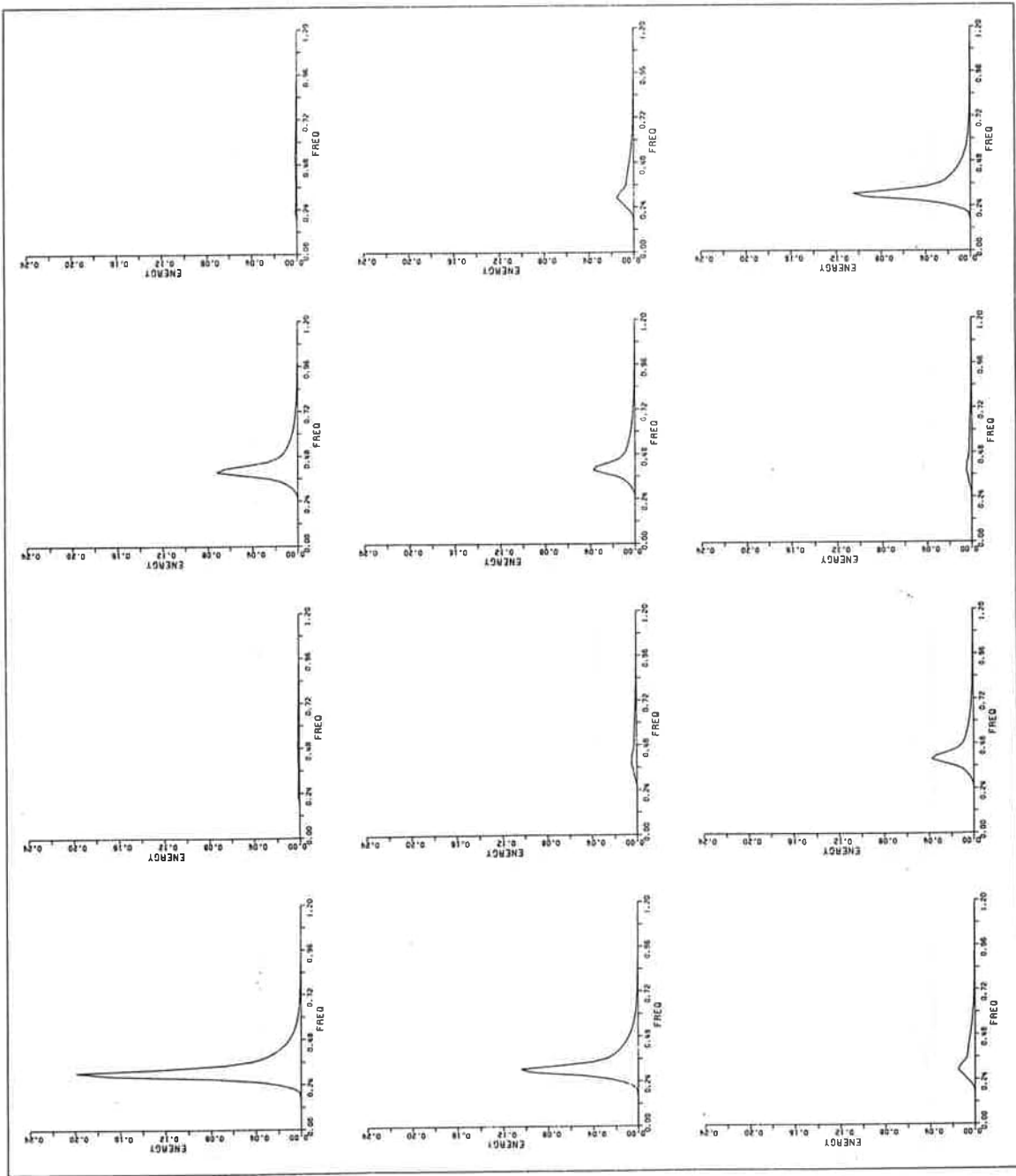


Fig. 14a  $E(f, \theta)$ :  $f_{1m} = 0.3\text{Hz}$ ,  $\theta_{1m} = 0^\circ$ ,  $f_{2m} = 0.4\text{Hz}$ ,  $\theta_{2m} = 180^\circ$

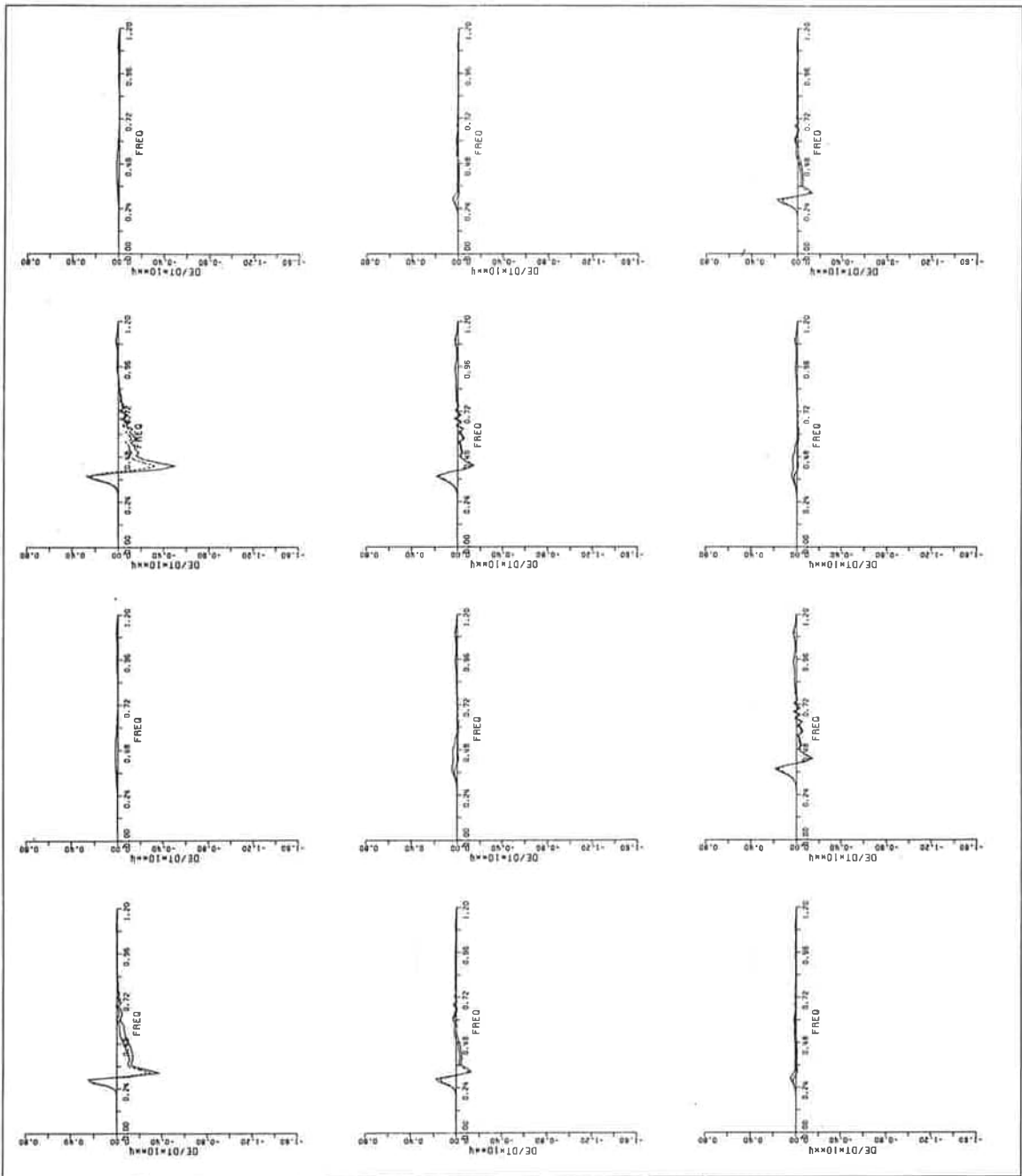


Fig. 14b  $S_{n1}(f, \theta)$

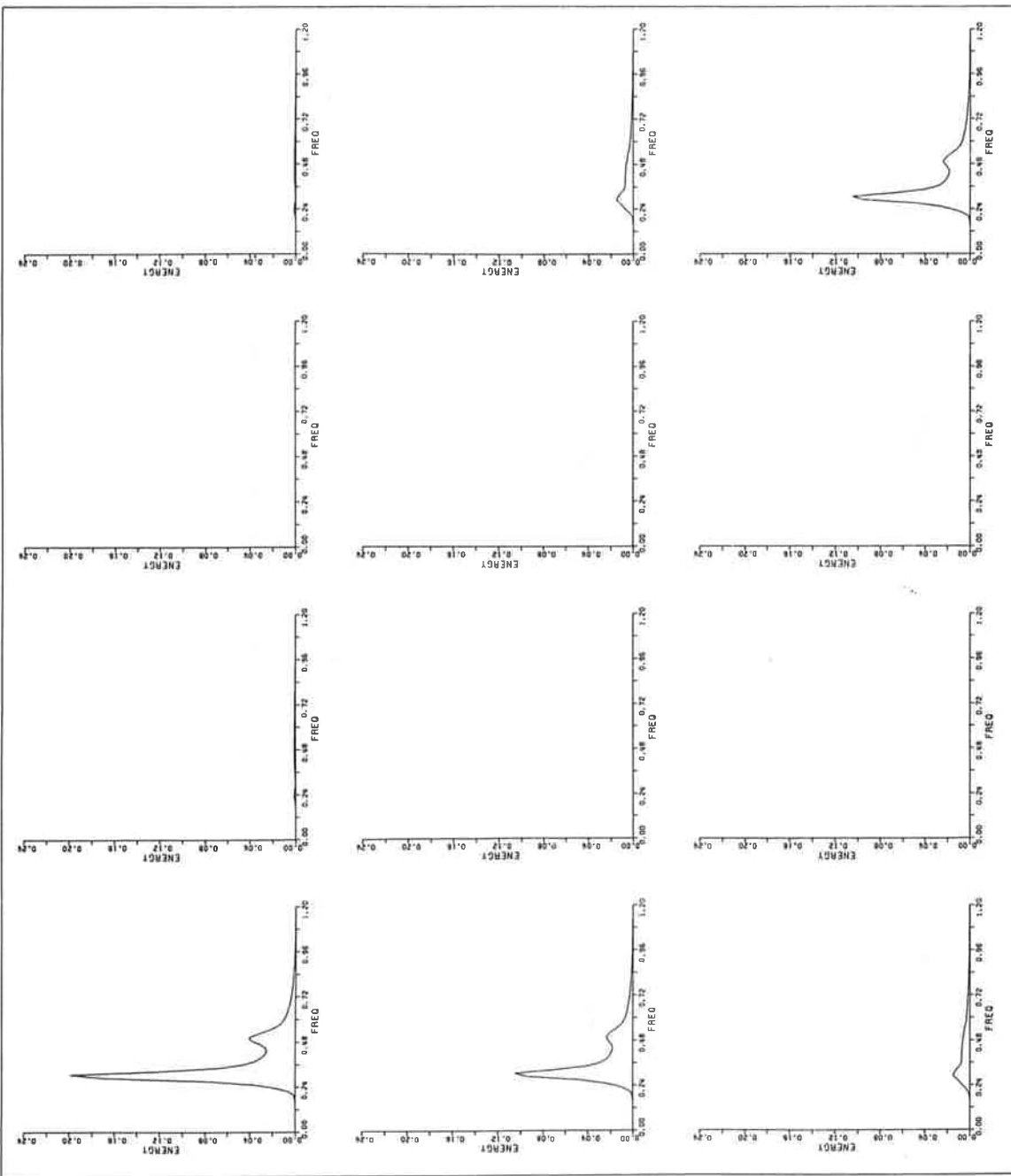
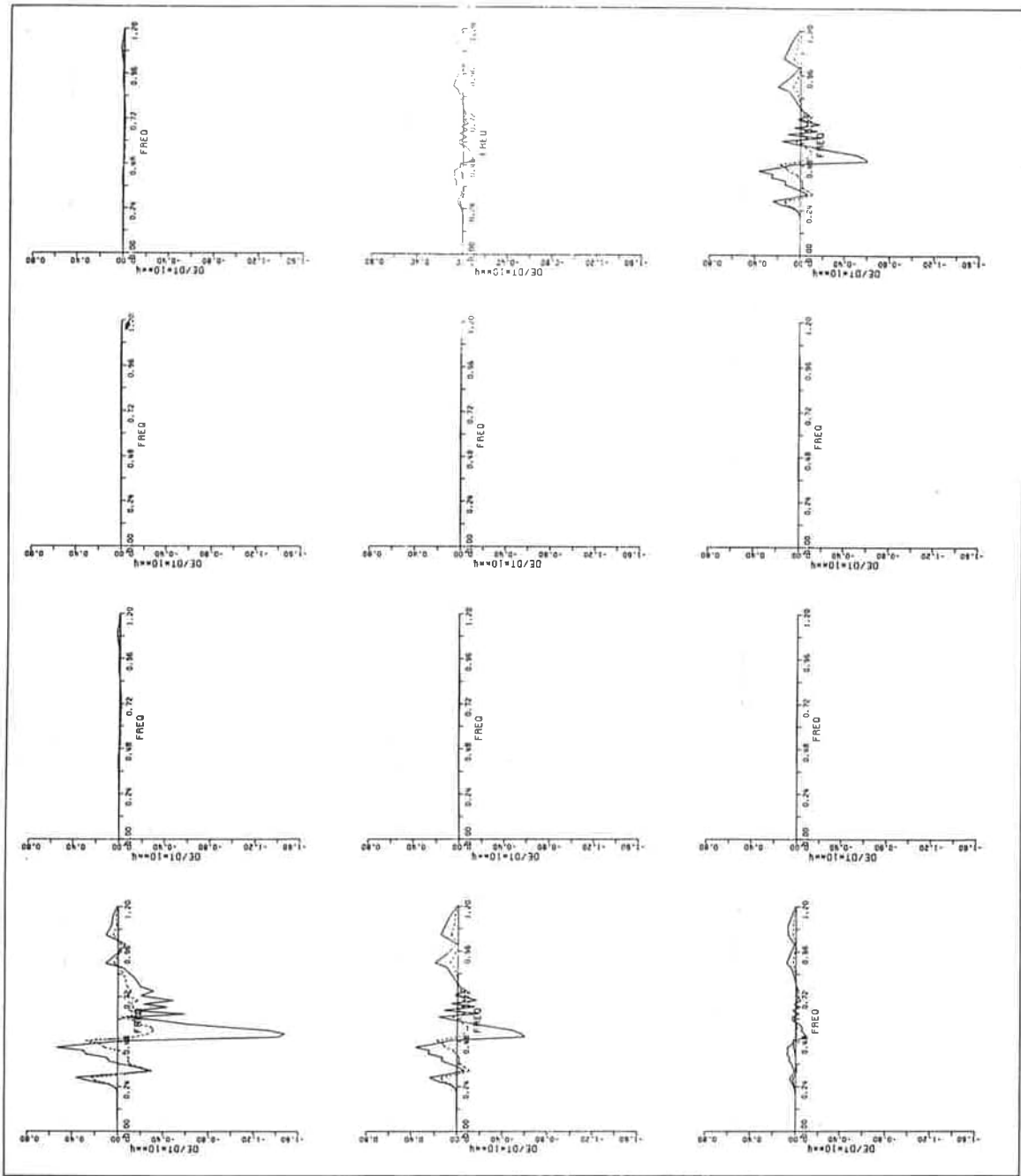


Fig. 15a  $E(f, \theta)$ :  $f_{1m} = 0.3\text{Hz}$ ,  $\theta_{1m} = 0^\circ$ ,  $f_{2m} = 0.5\text{Hz}$ ,  $\theta_{2m} = 0^\circ$

Fig. 15b  $S_{n1}(f, \theta)$



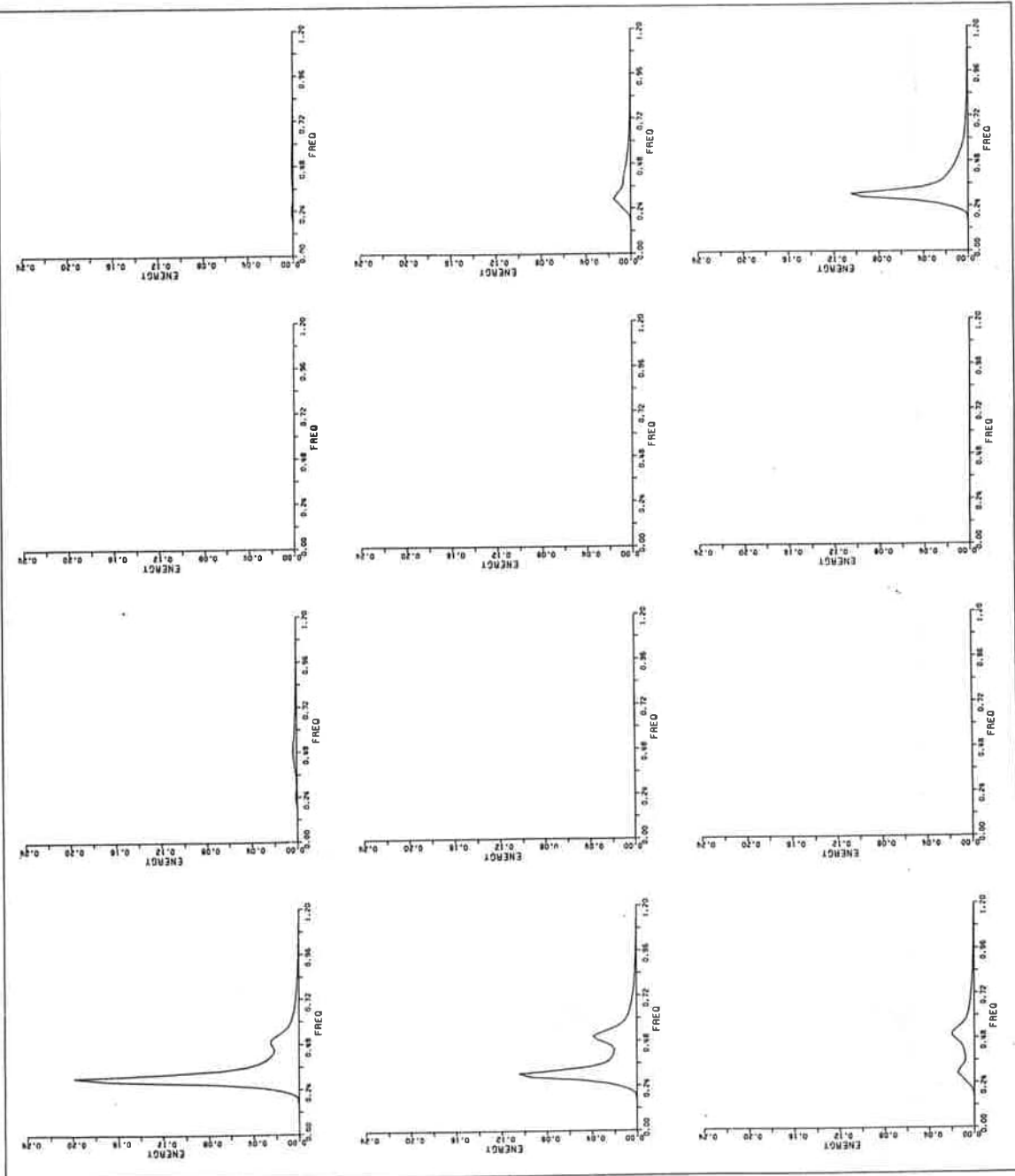


Fig. 16a  $E(f, \theta)$ :  $f_{1m} = 0.3\text{Hz}$ ,  $\theta_{1m} = 0^\circ$ ,  $f_{2m} = 0.5\text{Hz}$ ,  $\theta_{2m} = 30^\circ$

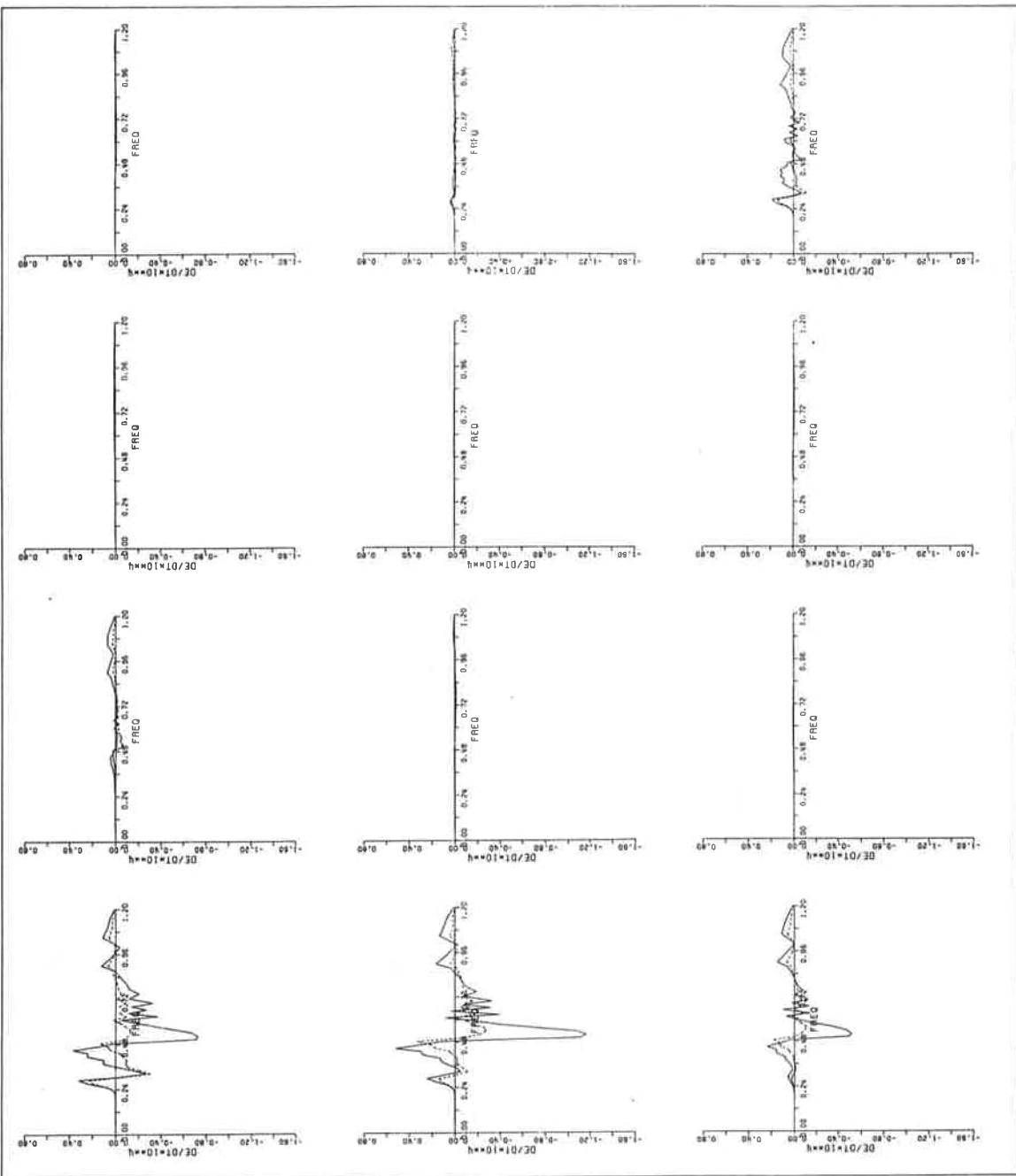


Fig. 16b  $S_{n1}(f, \theta)$

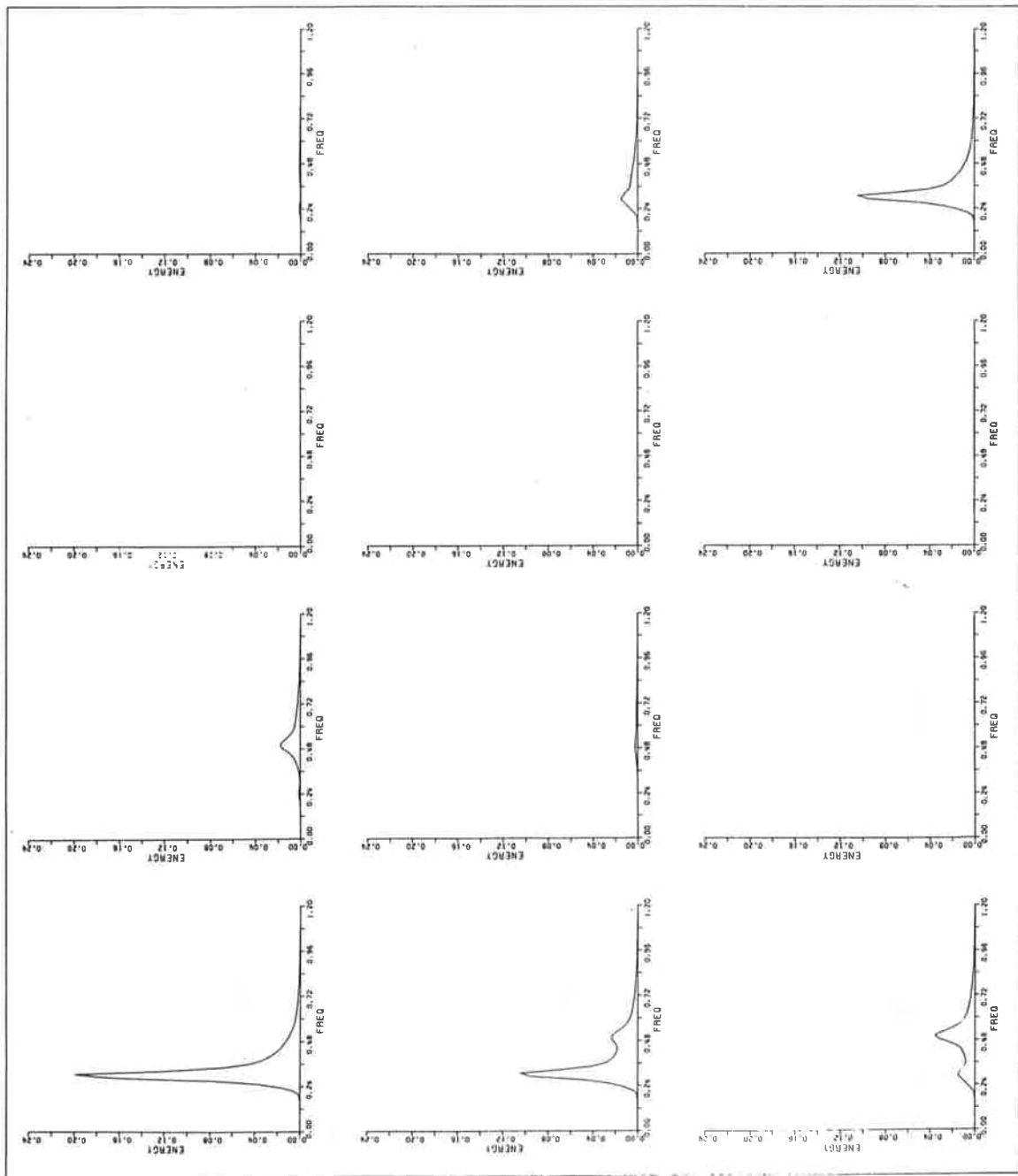


Fig. 17a  $E(f, \theta)$ :  $f_{1m} = 0.3\text{Hz}$ ,  $\theta_{1m} = 0^\circ$ ,  $f_{2m} = 0.5\text{Hz}$ ,  $\theta_{2m} = 60^\circ$

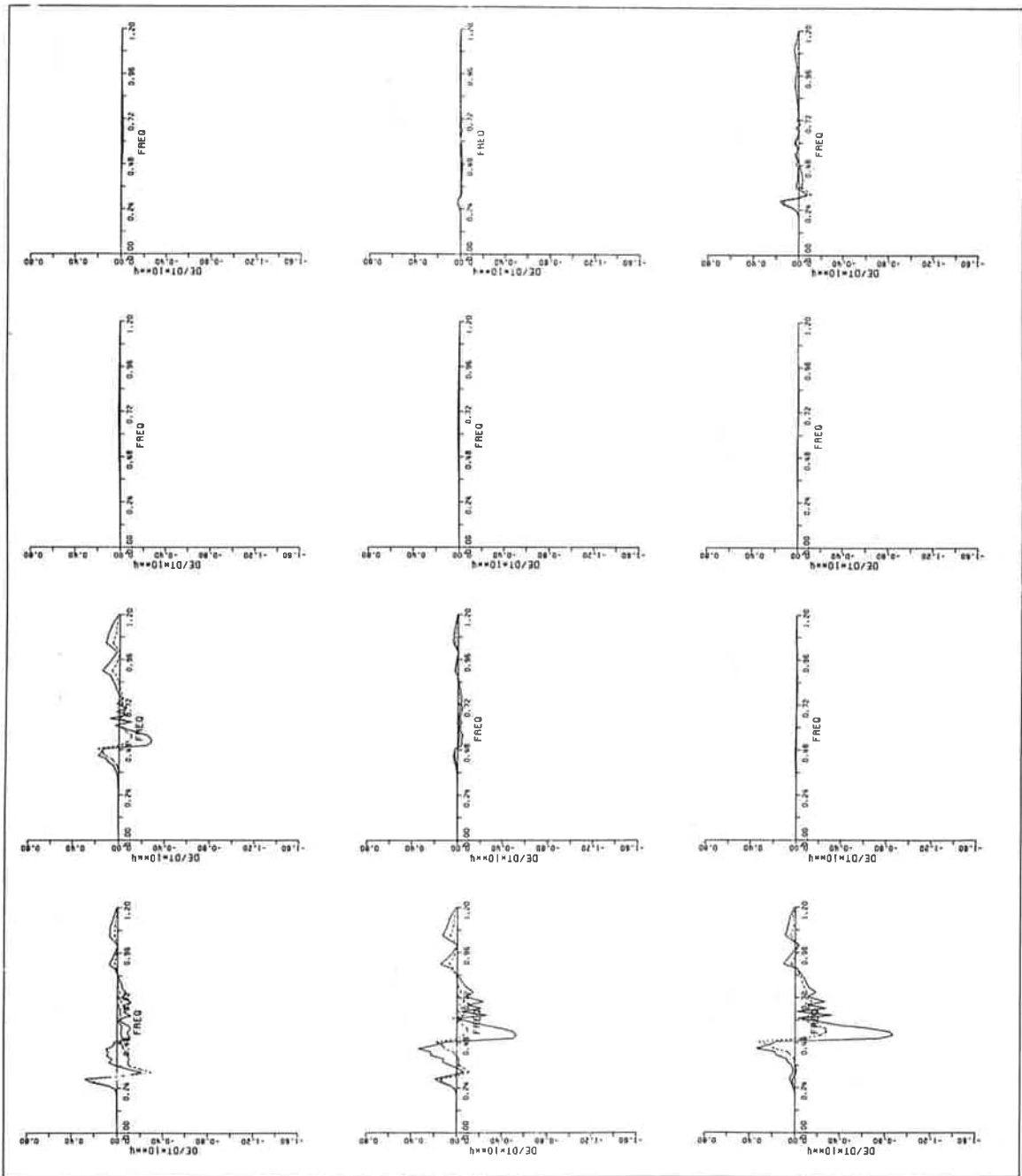


Fig. 17b  $S_{n1}$  ( $f, \theta$ )

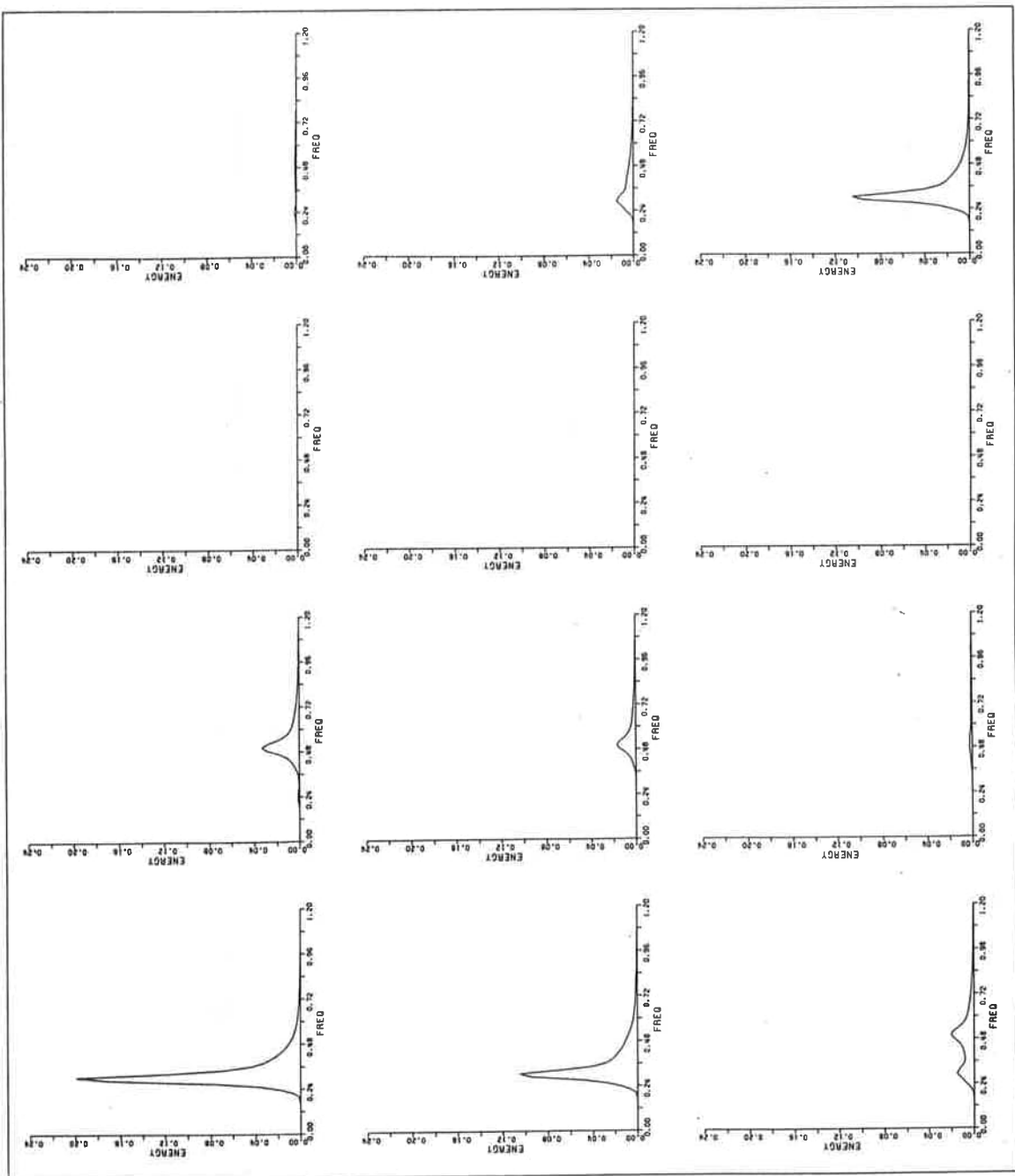


Fig. 18a  $E(f, \theta)$ :  $f_{1m} = 0.3\text{Hz}$ ,  $\theta_{1m} = 0^\circ$ ,  $f_{2m} = 0.5\text{ Hz}$ ,  $\theta_{2m} = 90^\circ$

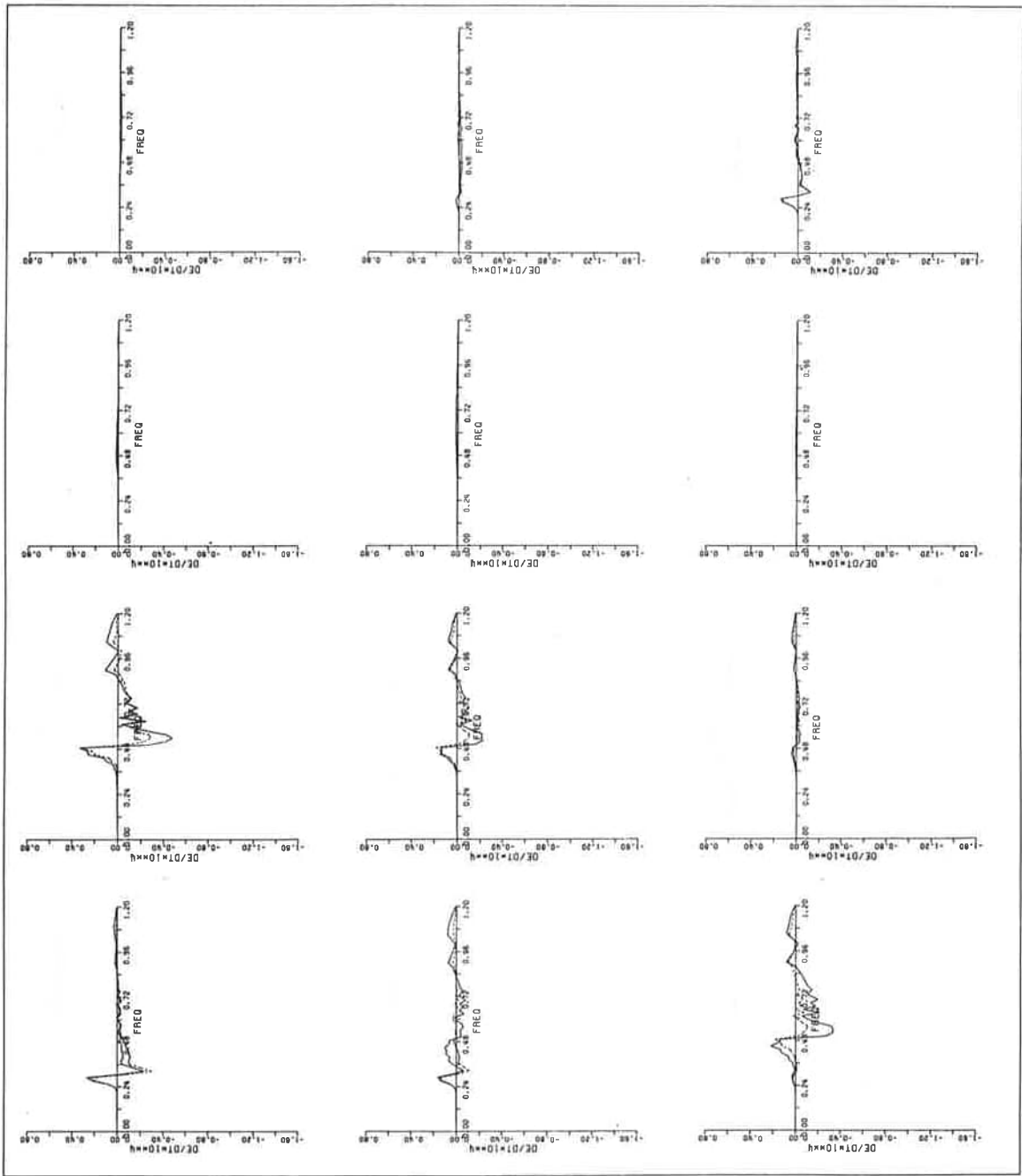


Fig. 18b  $S_{n1}(f, \theta)$

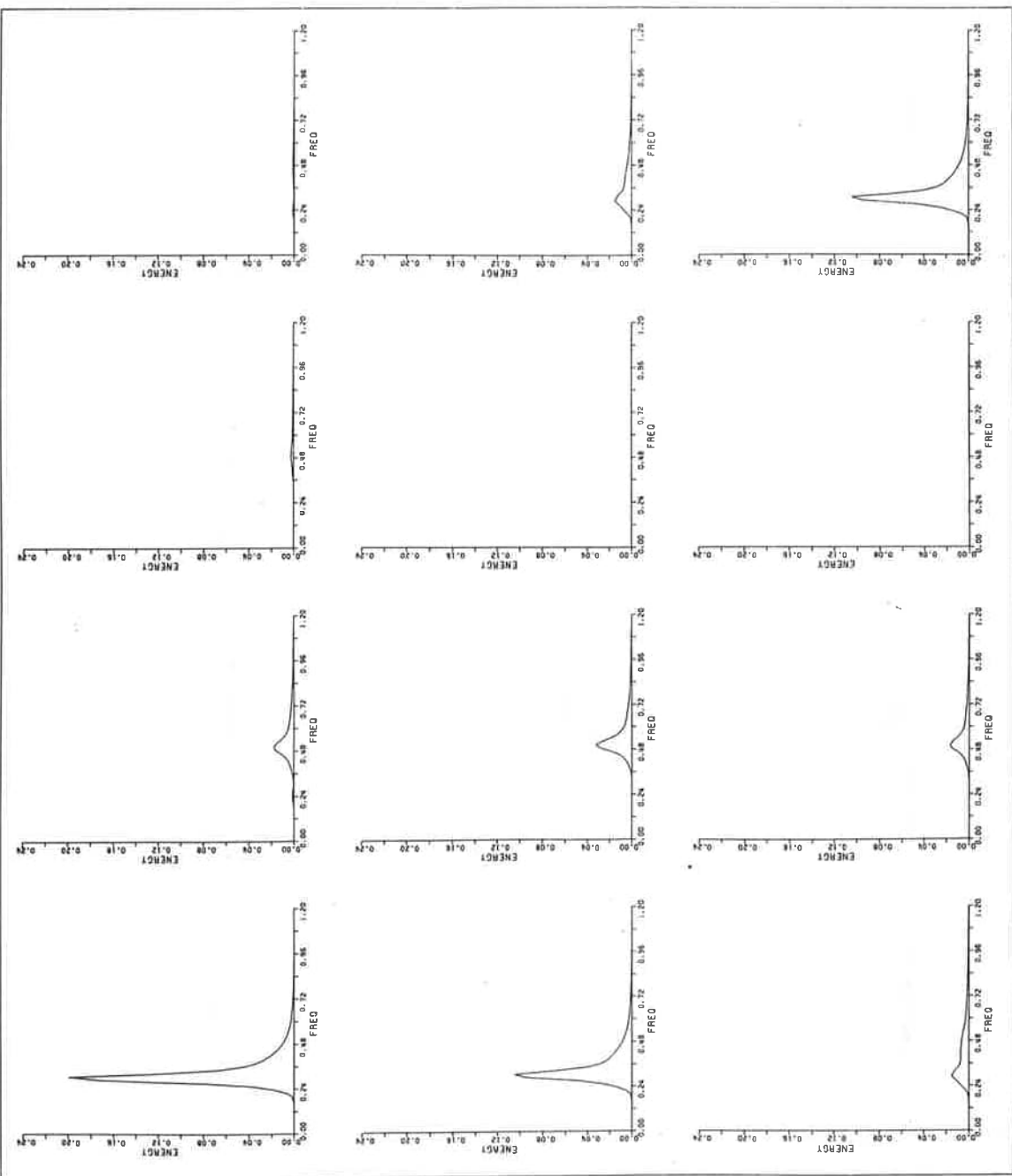


Fig. 19a  $E(f, \theta)$ :  $f_{1m} = 0.3\text{Hz}$ ,  $\theta_{1m} = 0^\circ$ ,  $f_{2m} = 0.5\text{Hz}$ ,  $\theta_{2m} = 120^\circ$

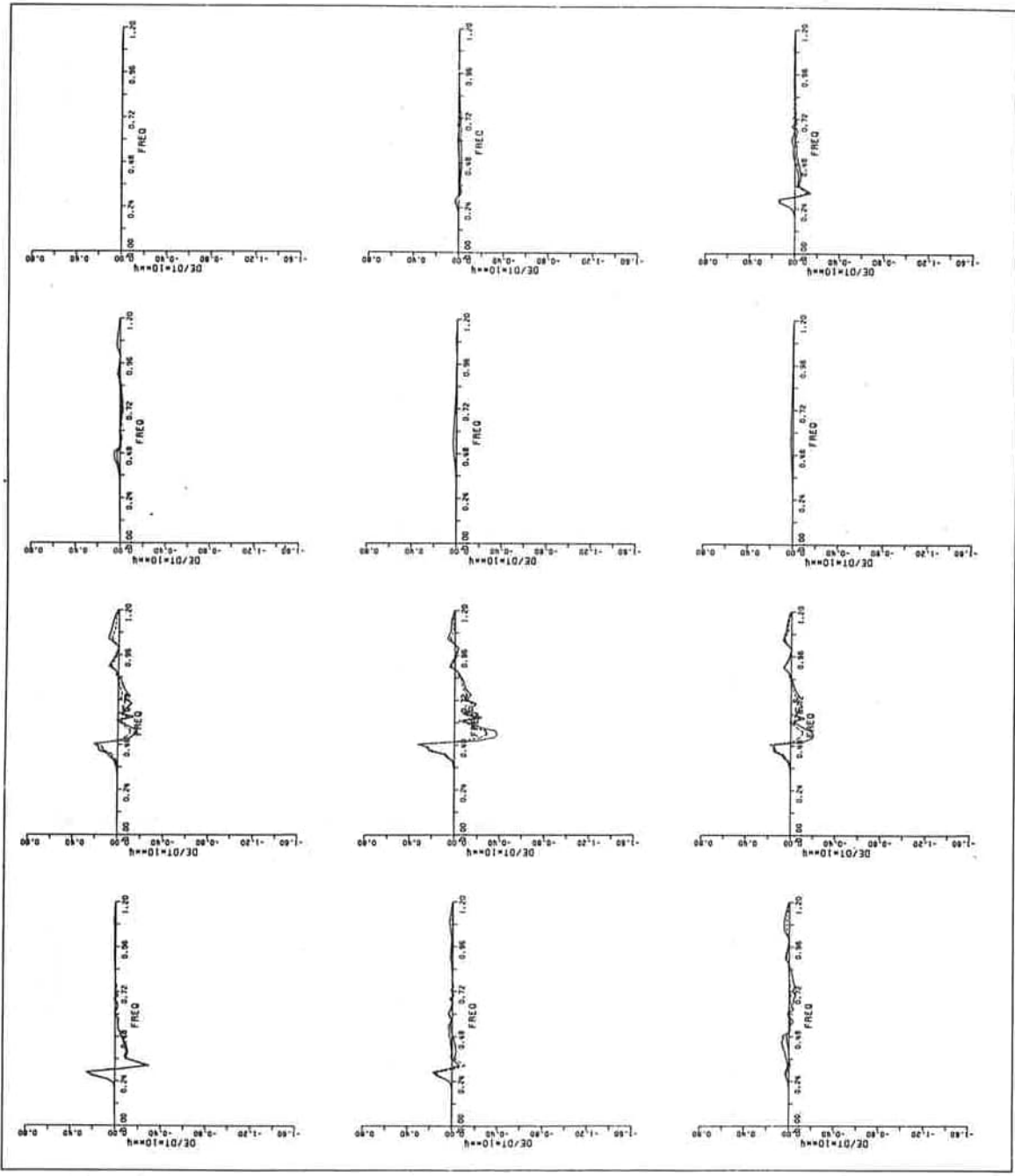


Fig. 19b  $S_{n1}(f, \theta)$

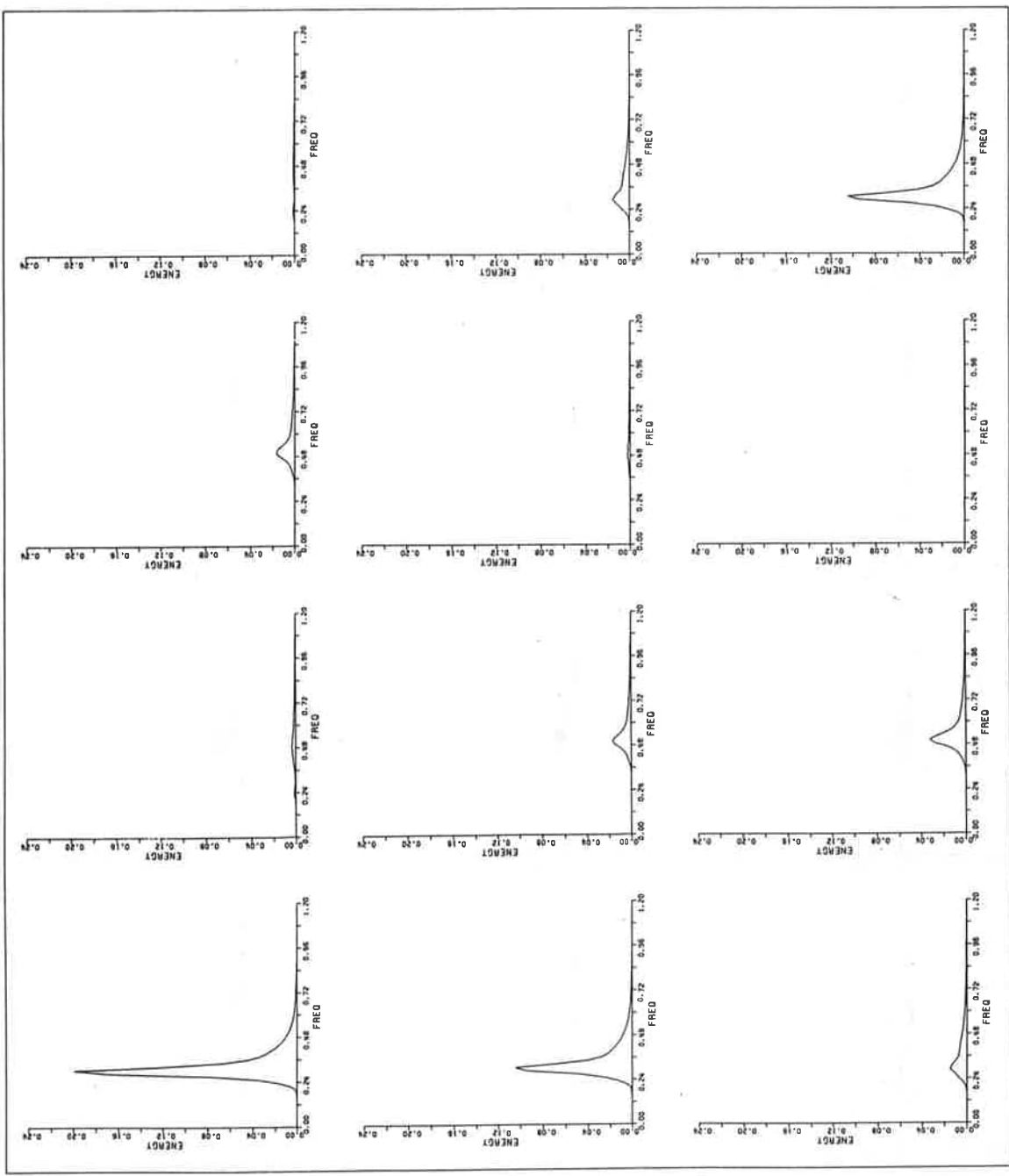
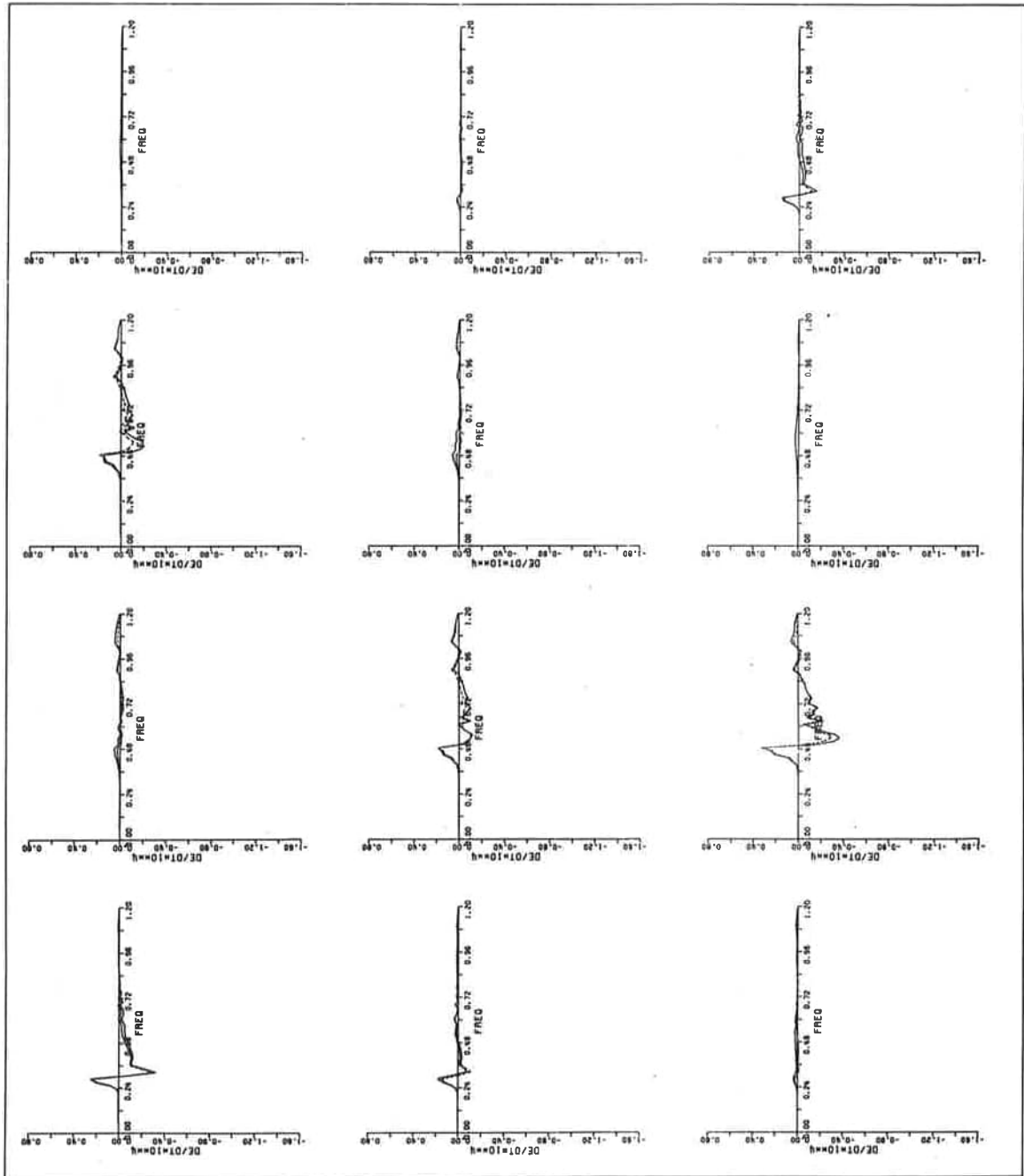


Fig. 20a  $E(f, \theta)$ :  $f_{1m} = 0.3\text{Hz}$ ,  $\theta_{1m} = 0^\circ$ ,  $f_{2m} = 0.5\text{Hz}$ ,  $\theta_{2m} = 150^\circ$

Fig. 20b  $S_{nl}(f, \theta)$



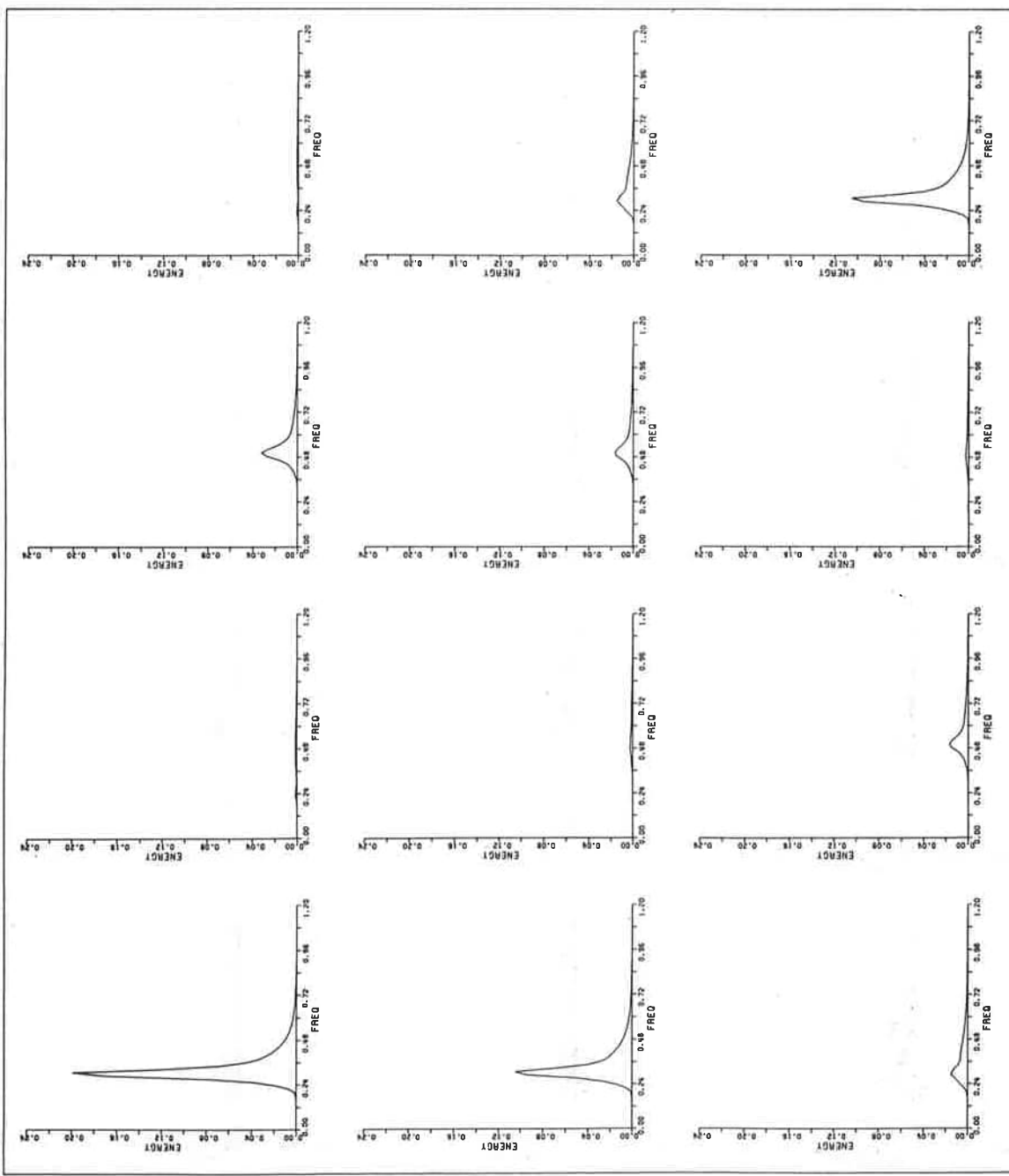


Fig. 21a  $E(f, \theta)$ :  $f_{1m} = 0.3\text{Hz}$ ,  $\theta_{1m} = 0^\circ$ ,  $f_{2m} = 0.5\text{Hz}$ ,  $\theta_{2m} = 180^\circ$

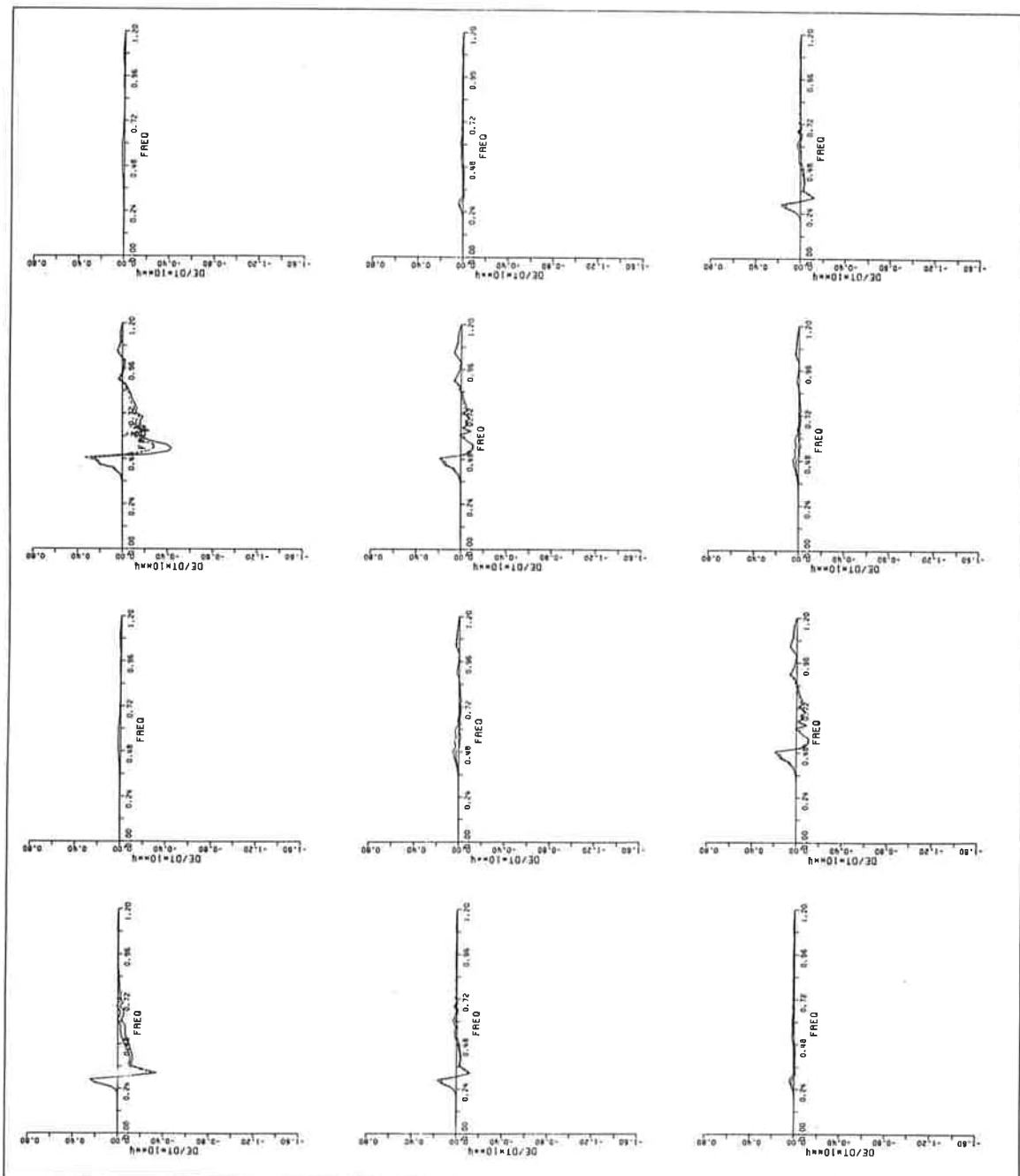


Fig. 21b  $S_{nl}(f, \theta)$